To the Graduate Council:

I am submitting herewith a thesis written by Christopher James Janke entitled "Synthesis, Characterization, and Electrochemical Studies on Some Selected Dinuclear Rhodium Complexes." I have examined the final copy of this thesis for form and content and recommend that it be accepted in partial fulfillment of the requirements for the degree of Master of Science, with a major in Chemistry.

Clifton Woods

Clifton Woods, III, Major Professor

We have read this thesis
and recommend its acceptance:

William E Bull

James Q. Chambers

Accepted for the Council:

Lawrence Dinkel

Vice Provost and
Dean of the Graduate School

STATEMENT OF PERMISSION TO USE

In presenting this thesis in partial fulfillment of the requirements for a Master's degree at The University of Tennessee, Knoxville, I agree that the Library shall make it available to borrowers under rules of the Library. Brief quotations from this thesis are allowable without special permission, provided that accurate acknowledgment of source is made.

Permission for extensive quotation from or reproduction of this thesis may be granted by my major professor, or in his absence, by the Head of Interlibrary Services when, in the opinion of either, the proposed use of the material is for scholarly purposes. Any copying or use of the material in this thesis for financial gain shall not be allowed without my written permission.

Signature Christopher J. Jaske

Date 2/18/86

SYNTHESIS, CHARACTERIZATION, AND ELECTROCHEMICAL STUDIES ON SOME SELECTED DINUCLEAR RHODIUM COMPLEXES

A Thesis

Presented for the

Master of Science

Degree

The University of Tennessee, Knoxville

Christopher James Janke

March 1986

DEDICATION

TO MOM, DAD, AND PAM

ACKNOWLEDGMENTS

I wish to express my gratitude to the Department of Chemistry, The University of Tennessee, Knoxville, for financial aid in the form of a graduate teaching/research assistantship and an Atlantic Richfield Foundation Fellowship.

I would like to express my special thanks to Dr. Clifton Woods, III for his guidance and support throughout my stay here at U-TK.

I would like to express my appreciation to the National Science Foundation for financial aid in the form of a research grant.

My very special thanks goes to my Mom and Dad for helping me through many financial binds.

Special thanks go to Tom, Louis, Dr. Clifton Woods, Dr. William Bull, and Dr. James Chambers.

I would also like to express my very special thanks to Jim and Imogene Burgess for treating me like their son and for making my stay here in Tennessee both pleasant and worthwhile.

Finally, a very special thanks to my future wife, Pamela Gail Burgess, for all her love and support.

ABSTRACT

New binuclear rhodium(I) complexes containing terminal carbon monoxide, bridging dpm (bis(diphenylphosphino)methane) ligands, and a triazolate anion or pyrazolate (pz) derivative in the bridgehead position have been investigated. Products obtained by the chemical oxidation of these complexes using I_2, Br_2, and Cl_2 have also been synthesized. It has been found that with some of the pz derivatives that are not substituted in the 4-position treatment of Br_2 and Cl_2 with some of the complexes leads to substitution in the 4-position as well as oxidative addition at the metal centers.

The electrochemical behavior of several rhodium complexes has been examined using cyclic voltammetry and bulk electrolysis. A new Rh(II)-Rh(II) complex has been prepared by the electrochemical oxidation of a methylene chloride solution containing trans-$Rh_2Cl_2(CO)_2(dpm)_2$ in the presence of excess chloride to give the compound, $[Rh_2Cl_2(\mu\text{-}CO)(\mu\text{-}Cl)(dpm)_2]PF_6$, 4. This new product when treated with CO undergoes simultaneous substitution, addition, and reduction reactions to produce a mixture of Rh(I)-Rh(I) and Rh(II)-Rh(II) dimers.

TABLE OF CONTENTS

CHAPTER		PAGE
I.	INTRODUCTION	1
	A. Literature Review	1
	B. Statement of Purpose	22
II.	EXPERIMENTAL	24
	A. Chemicals	24
	1. Solvents	24
	2. Reagents	25
	3. Miscellaneous	26
	B. Spectroscopy	28
	1. Infrared spectroscopy	28
	2. Ultraviolet-visible spectroscopy	28
	3. Nuclear magnetic resonance spectroscopy (NMR)	28
	C. Electrochemistry	29
	1. Bulk electrolysis, coulometry, and cyclic voltammetry	29
	2. Electrodes	29
	3. Cells	30
	D. Elemental Analysis	30
	1. μ-Carbonyldicarbonyl-μ-chlorobis[μ-methylenebis-[diphenylphosphine]-P:P']-dirhodium(I) hexafluorophosphate, $[Rh_2(CO)_3Cl(dpm)_2][PF_6]$	30
	2. Dicarbonyl-μ-chlorobis[μ-methylenebis[diphenylphosphine]-P:P']-dirhodium(I) hexafluorophosphate, $[Rh_2(CO)_2Cl(dpm)_2][PF_6]$	31
	3. <u>trans</u>-Dicarbonyldichlorobis[μ-methylenebis[diphenylphosphine]-P:P'-dirhodium(I), $Rh_2(CO)_2Cl_2(dpm)_2$	31
	4. μ-Carbonyl-μ-chlorodichlorobis[μ-methylenebis[diphenylphosphine]-P:P'-dirhodium(II) hexafluorophosphate, $[Rh_2(CO)Cl_3(dpm)_2][PF_6]$	32
	5. Trichloro-μ-chlorocarbonylbis[μ-methylenebis[diphenylphosphine[-P:P']-dirhodium(II), $[Rh_2Cl_4(CO)(dpm)_2]$	33
	6. Dicarbonyl-μ-3,5-dimethylpyrazolatobis[μ-methylenebis[diphenylphosphine]-P:P']-dirhodium(I) hexafluorophosphate, $[Rh_2(CO)_2(C_5H_7N_2)(dpm)_2][PF_6]$	33

CHAPTER PAGE

II. (CONTINUED)

7. Dicarbonyl-μ-pyrazolatobis[μ-methylenebis[diphenylphosphine]-P:P']-dirhodium(I) hexafluorophosphate, $[Rh_2(CO)_2(C_3H_3N_2)(dpm)_2]$-$[PF_6]$. 34
8. Dicarbonyl-μ-4-methylpyrazolatobis[μ-methylenebis[diphenylphosphine]-P:P']-dirhodium(I) hexafluorophosphate, $[Rh_2(CO)_2(C_4H_5N_2)(dpm)_2][PF_6]$. 35
9. Dicarbonyl-μ-triazolatobis[μ-methylenebis[diphenylphosphine]-P:P']-dirhodium(I) hexafluorophosphate, $[Rh_2(CO)_2(C_2H_2N_3)(dpm_2)]$-$[PF_6]$. 35
10. Dicarbonyldiiodo-μ-3,5-dimethylpyrazolatobis[μ-methylenebis[diphenylphosphine]-P:P']-dirhodium(II) hexafluorophosphate, $[Rh_2(CO)_2I_2(C_5H_7N_2)(dpm)_2][PF_6)$. 36
11. Dicarbonyldiiodo-μ-pyrazolatobis[μ-methylenebis[diphenylphosphine]-P:P']-dirhodium(II) hexafluorophosphate, $[Rh_2(CO)_2I_2(C_3H_3N_2)(dpm)_2]$-$[PF_6]$. 37
12. Dicarbonyliiodo-μ-4-methylpyrazolatobis[μ-methylenebis[diphenylphosphine]-P:P']-dirhodium (II) hexafluorophosphate, $(RH_2(CO)_2I_2(C_4H_5N_2)(dpm)_2][PF_6]$. 37
13. Dicarbonyldiiodo-μ-triazolatibos[μ-methylenebis[diphenylphosphine]-P:P']-dirhodium(II) hexafluorophosphate, $[Rh_2(CO)_2I_2(C_2H_2N_3)(dpm)_2][PF_6]$. 38
14. Dibromodicarbonyl-μ-4-bromo-pyrazolatobis[μ-methylenebis[diphenylphosphine]-P:P']-dirhodium(II) hexafluorophosphate, $[Rh_2Br_2(CO)_2(C_3H_2BrN_2)(dpm)_2][PF_6]$ 38
15. Dibromodicarbonyl-μ-4-bromo-3,5-dimethyl-pyrazolatobis[μ-methylenebis[diphenylphosphine]-P:P']-dirhodium(II) hexafluorophosphate, $[Rh_2Br_2(CO)_2(C_5H_6BrN_2)(dpm)_2[PF_6]$ . . . 39
16. Dibromodicarbonyl-μ-4-methylpyrazolatobis[μ-methylenebis[diphenylphosphine]-P:P']-dirhodium(II) hexafluorophosphate, $[Rh_2Br_2(CO)_2(C_4H_5N_2)(dpm)_2][PF_6]$ 40
17. Dicarbonyldichloro-μ-4-chloro-pyrazolatobis[μ-methylenebis[diphenylphosphine[-P:P']-dirhodium(II) hexafluorophosphate, $[Rh_2(CO)_2Cl_2(C_3H_2ClN_2)(dpm)_2][PF_6]\cdot.25\ CH_2Cl_2$. 40

CHAPTER PAGE

II. (CONTINUED)

18. Dicarbonyldichloro-μ-4-chloro-3,5-dimethylpyrazolatobis[μ-methylenebis[diphenylphosphine]-P:P']-dirhodium(II) hexafluorophosphate, $[Rh_2(CO)_2Cl_2(C_5H_6ClN_2)(dpm)_2][PF_6]\cdot .25\ CH_2Cl_2$ 41
19. Dicarbonyldichloro-μ-4-methylpyrazolatobis[μ-methylenebis[diphenylphosphine]-P:P']-dirhodium(II) hexafluorophosphate, $[Rh_2(CO)_2Cl_2(C_4H_5N_2)(dpm)_2][PF_6]\cdot .25\ CH_2Cl_2$. 41
20. Dicarbonyl-μ-4-bromo-3,5-dimethylpyrazolatobis[μ-methylenebis[diphenylphosphine]-P:P']-dirhodium(I) hexafluorophosphate, $[Rh_2(CO)_2(C_5H_6BrN_2)(dpm)_2][PF_6]$. 42
21. Dicarbonyl-μ-4-chloro-3,5-dimethylpyrazolatobis[μ-methylenebis[diphenylphosphine]-P:P']-dirhodium(I) hexafluorophosphate, $[Rh_2(CO)_2(C_5H_6ClN_2)(dpm)_2][PF_6]\cdot .25\ CH_2Cl_2$. . 43

III. RESULTS AND DISCUSSION. 44

IV. ELECTROSYNTHESIS OF RHODIUM(II) COMPLEXES 70

V. CONCLUSIONS 78

LIST OF REFERENCES. 80

VITA. 83

LIST OF TABLES

TABLE		PAGE
I.	Compound Identification.	45
II.	$^{31}P\ \{^{1}H\}$ NMR Spectral Data for Selected Compounds 6-11 .	48
III.	UV-Vis Spectral Data for Selected Compounds 6-11	50
IV.	UV-Vis Spectral Data in the 500-515 nm Range for Selected Compounds	53
V.	IR Spectral Data for Selected Compounds.	54
VI.	$^{31}P\ \{^{1}H\}$ NMR Spectral Data for Selected Compounds 16-19.	57
VII.	$^{31}P\ \{^{1}H\}$ NMR Spectral Data for Selected Compounds 24-29.	59
VIII.	UV-Vis Spectral Data for Selected Compounds 24-29. . . .	61
IX.	Cyclic Voltammetric Data for the Complexes, 6-9.	67

LIST OF FIGURES

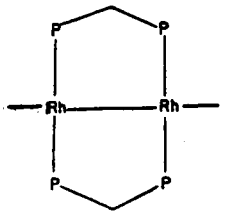
FIGURE		PAGE
1.	The $^{31}P\{^{1}H\}$ NMR Spectrum of $[Rh_2(CO)_2(\mu\text{-}3,5\text{-DMP})(dmp)_2]\text{-}PF_6$, 6.	47
2.	Simplified Molecular Orbital Diagram Showing the Orbital Interactions Resulting from Face-to-Face Approach of Two Square-Planar Rh(I) Units	51
3.	Oxidation of the Hexafluorophosphate and Perchlorate Complexes, 6-15, by Molecular Iodine (1:1 Mol Ratio) to Form the Complexes, 16-23	52
4.	Products Obtained from Bromination or Chlorination of Complexes, 6-8.	62
5.	The $^{31}P\{^{1}H\}$ NMR Spectrum of $[Rh_2Br_2(CO)_2(\mu\text{-}4B\text{-}pz)(dpm)_2]\text{-}PF_6$, 24	65
6.	Cyclic Voltammogram of 8.	66
7.	Cyclic Voltammogram of 3 with Excess TBACl.	71
8.	Cyclic Voltammogram of 3 with Excess TBACl after Oxidation at +0.70 Volts.	72
9.	The $^{31}P\{^{1}H\}$ NMR spectrum of $Rh_2Cl_3(CO)(\mu\text{-}Cl)(dpm)_2$, 5.	75

CHAPTER I

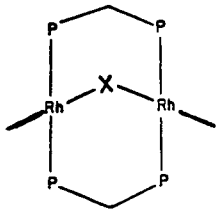
INTRODUCTION

A. Literature Review

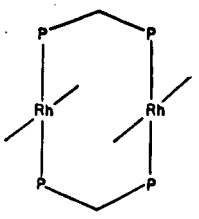
Binuclear rhodium complexes in which both metals are held in close proximity by two bridging dpm (bis(diphenylphosphino)methane) ligands have received considerable attention in recent years. Complexes of this type can be divided into four classes:



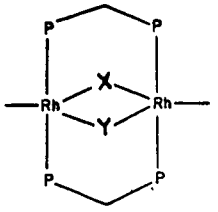
Side-by-Side



A-Frame



Face-to-Face

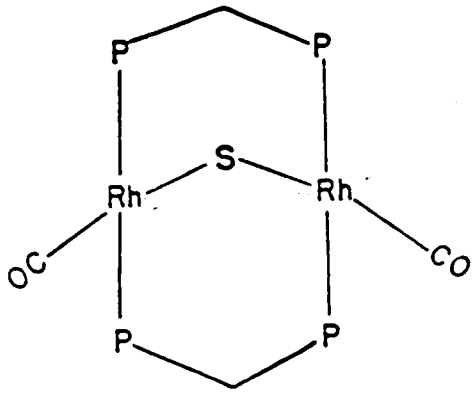


Double A-Frame

One particular interesting class are the A-frame complexes which have the ability to coordinate ligands including carbon monoxide, sulfur dioxide, halides, and acetylenes into the bridgehead position. Many A-frame complexes exhibit significant catalytic activity in the hydrogenation of acetylenes and olefins, and in the water gas shift reaction.

This catalytic activity is exemplified by the neutral A-frame complex, $Rh_2Cl_2(\mu\text{-}CO)(dpm)_2$, which was shown in a recent study to catalyze the hydrogenation of diphenylacetylene and phenylacetylene in methanol.[1] These electron-releasing acetylenes are believed to activate the A-frame complex toward the oxidative addition of hydrogen, which is considered to be a necessary step in the hydrogenation reaction. It was also shown that the hydrogenation of the highly electron-withdrawing DMA (dimethylacetylenedicarboxylate) does not occur since this acetylene serves to deactivate the complex. However, $Rh_2Cl_2(\mu\text{-}CO)(dpm)_2$ does catalyze the cyclotrimerization of DMA in methanol to form hexamethyl mellitate.

The first Rh(I) dimer having the A-frame type structure,



was reported by R. Eisenberg in 1977.[2] This red crystalline complex, $Rh_2(CO)_2(\mu\text{-}S)(dpm)_2$, was prepared by adding Na_2S to a methanolic suspension of <u>trans</u>-$Rh_2(CO)_2Cl_2(dpm)_2$ followed by the precipitation of an analytically pure product. The complex exhibits two terminal carbonyl stretching frequencies of 1920 (vs) and 1933 (s) cm^{-1} with

a sulfide ligand occupying the bridgehead position. This A-frame species possesses C_2 symmetry, has a dihedral angle of 83.3° between the two square planes, and a Rh---Rh separation of 3.155 Å.[2]

$Rh_2(CO)_2(\mu\text{-}S)(dpm)_2$ undergoes substitution reactions as well as reactions with electrophilic reagents. Upon addition of MeNC to the dimer, the immediate evolution of CO occurs with the formation of an analogous species, $Rh_2(CNMe)_2(\mu\text{-}S)(dpm)_2$. The reactivity of the bridging sulfide is exemplified by the reaction of the electrophilic reagent, $(OEt_3)PF_6$, with $Rh_2(CO)_2(\mu\text{-}S)(dpm)_2$ to form the cationic dimer, $[Rh_2(CO)_2(\mu\text{-}SEt)(dpm)_2]PF_6$.[2] Other electrophilic species including H^+ and $PhCH_2^+$ react with the complex to form similar sulfur alkylated cationic A-frame complexes. The addition of a strong base to the complex, $Rh_2(CO)_2(\mu\text{-}SH)(dpm)_2^+$, produces the starting complex, $Rh_2(CO)_2(\mu\text{-}S)(dpm)_2$.[3]

An interesting reaction displaying the lability of the bridging sulfide involves the treatment of $Rh_2(CO)_2(\mu\text{-}S)(dpm)_2$ with either MeI or EtI and subjecting it to CO yielding the product, $[Rh_2(CO)_2(\mu\text{-}I)(\mu\text{-}CO)(dpm)_2]I$.[3] This reaction is believed to occur by the loss of the bridged monoalkylated sulfide with addition of iodide and CO into the bridging positions. The starting complex can be regenerated by the addition of Na_2S to this double A-frame complex.[2]

In 1977 Balch reported the first case of an A-frame complex containing a bridging reversible bonding CO. This dark red crystalline Pd(I) dimer, $Pd_2X_2(\mu\text{-}CO)(dpm)_2$ (X = Cl, Br), readily loses

bridging CO when refluxed in a methylene chloride solution or when heated to 56°C under vacuum forming the metal-metal bonded dimer, $Pd_2X_2(dpm)_2$ (X = Cl, Br).[4]

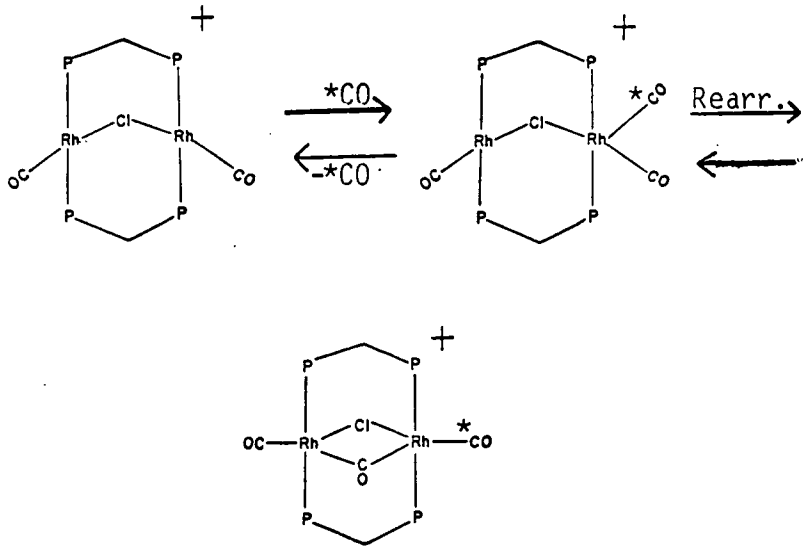
The first structurally characterized example of a metal-metal bonded Rh(I) dimer having a double A-frame structure featuring a bridging chloride and a reversible binding bridging carbonyl ligand was reported by Cowie, Mague, and Sanger in 1978.[5] This complex, $[Rh_2(CO)_2(\mu\text{-}Cl)(\mu\text{-}CO)(dpm)_2]BPh_4$, was prepared by the addition of equimolar quantities of dpm and $NaBPh_4$ to an ethanolic solution of $[Rh(CO)_2Cl_2]^-$ under CO followed by recrystallization from a chloroform-ethanol mixture. The yellow complex exhibits three carbonyl stretching frequencies at 1992 (s), 1977 (vs), and 1863 (s) cm^{-1} (Nujol mull), and has been shown by ^{31}P NMR to possess an AA'A"A'"XX' spin system ($\delta(P)$ = 25.5 ppm vs external 85% H_3PO_4) indicating the chemical equivalance of all four phosphorus atoms.

The structure of this complex involves a distorted trigonal-bipyramidal arrangement of ligands around each Rh atom with a Rh-Rh distance of 2.842 Å. Evidence suggesting the presence of a metal-metal bond include: (1) the acute angles at the two bridging ligands (Rh-Cl-Rh, 66.4° and Rh-C-Rh 87.7°), (2) the significantly longer intraligand distance of P---P compared to the Rh-Rh distance (3.396 Å compared to 2.842 Å), and (3) the diamagnetic behavior of the complex.[5] In $[Rh_2(CO)_2(\mu\text{-}Cl)(\mu\text{-}CO)(dpm)_2]BPh_4$, as with most other A-frame complexes containing bridging dpm ligands, the methylene groups attached to the dpm ligands are oriented in a cis

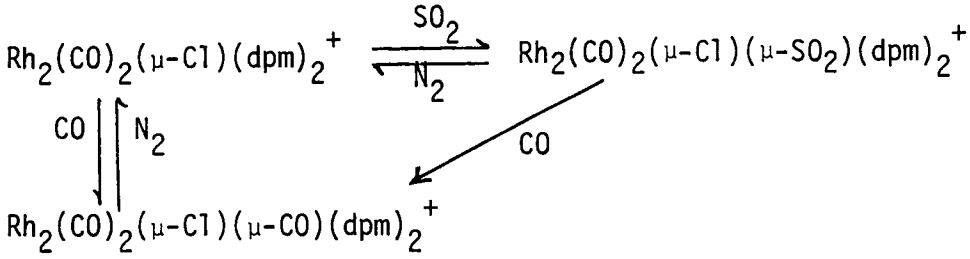
arrangement and are folded toward the larger ligand (the chloride ligand in this case). This minimizes the non-bonded contacts involving the more bulky phenyl rings and the ligands situated in the equatorial plane.[6]

The novelty of this complex arises from the fact that it contains a reversible bonding bridging carbonyl ligand in the active site opposite the bridging chloride. Dissolution of this complex in either acetone or methylene chloride, followed by bubbling the solution with N_2 or Ar, leads to the following complex, $[Rh_2(CO)_2(\mu\text{-}Cl)(dpm)_2]BPh_4$. If a solution of this latter complex is bubbled with carbon monoxide, the original complex, $[Rh_2(CO)_2(\mu\text{-}Cl)(\mu\text{-}CO)(dpm)_2]BPh_4$, is regenerated.[5]

The mechanism involved in this reversible carbonyl process was elucidated by exchange experiments using C-13 enriched CO. These experiments showed that all the carbonyl ligands present in both the dicarbonyl and tricarbonyl species are readily exchanged. By subjecting a solution of $[Rh_2(CO)_2(\mu\text{-}Cl)(dpm)_2]BPh_4$ to ^{13}CO at -70°C and monitoring the exchange process using infrared spectroscopy it was shown that the ^{13}CO initially attacks the complex at the terminal site between the bridging chloride and the terminal carbonyl ligand. This is followed by a rearrangement of the terminal CO cis to the ^{13}CO into a bridging position. This process continues until $[Rh_2(CO)_2(\mu\text{-}Cl)(\mu\text{-}CO)(dpm)_2]BPh_4$ is completely enriched with ^{13}CO. The rapid interconversion, dicarbonyl $\rightleftarrows$ tricarbonyl, occurs via bridge-terminal exchange which is illustrated below.[5]



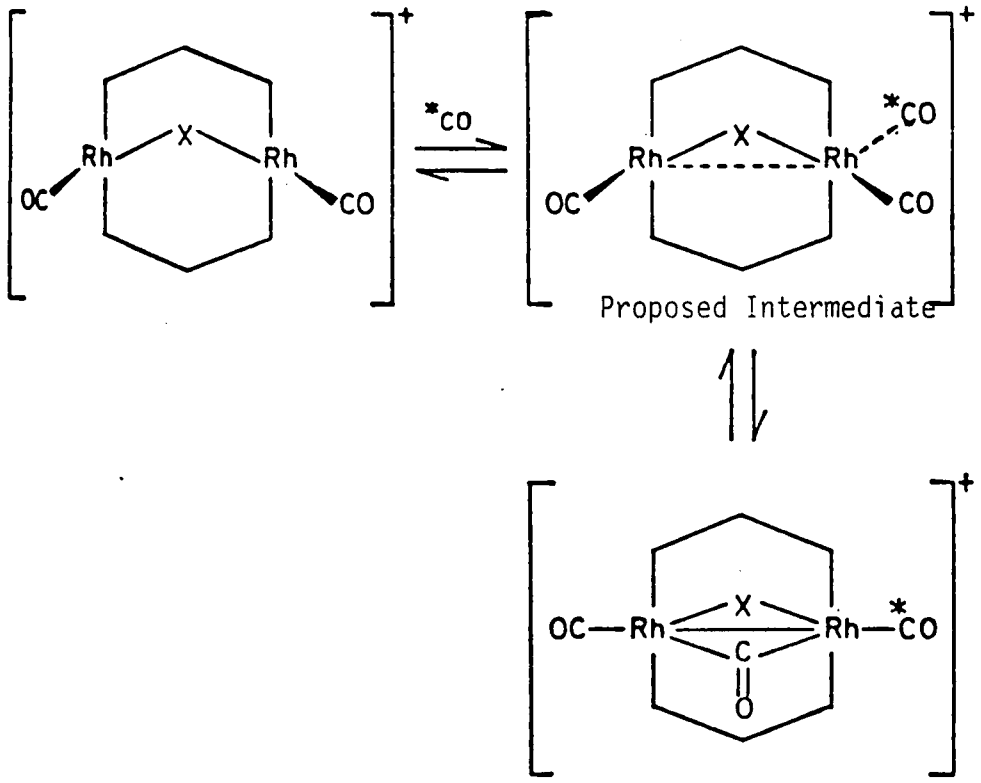
Another cationic double A-frame complex having a reversible binding bridging ligand situated in the active site is $[Rh_2(CO)_2(\mu\text{-}Cl)(\mu\text{-}SO_2)(dpm)_2]BPh_4$. This complex is synthesized by bubbling an acetone or methylene chloride solution (containing traces of chloride[7]) of $[Rh_2(CO)_2(\mu\text{-}Cl)(dpm)_2]BPh_4$ with SO_2. The lability of the bridging CO and SO_2 ligands situated in the active sites in the complexes, $[Rh_2(CO)_2(\mu\text{-}Cl)(\mu\text{-}CO)(dpm)_2]BPh_4$ and $[Rh_2(CO)_2(\mu\text{-}Cl)(\mu\text{-}SO_2)(dpm)_2]BPh_4$, respectively, is shown below.[8]



The weakly bound bridging CO in the tricarbonyl (solid) is further demonstrated by the loss of the bridging CO ligand to form <u>cis</u>-$Rh_2(CO)_2Cl_2(dpm)_2$ when chloride is the counterion.[8]

The formation of the complexes, $[Rh_2(CO)_2(\mu\text{-}Cl)(\mu\text{-}CO)(dpm)_2]BPh_4$ and $[Rh_2(CO)_2(\mu\text{-}Cl)(\mu\text{-}SO_2)(dpm)_2]BPh_4$, proceeds by two different routes. In the former complex CO attacks between the bridging chloride and terminal CO ligand, whereas in the latter complex the SO_2 attacks directly at the active site. There seems to be no obvious reason for this.[8]

Cationic double A-frame complexes analogous to $Rh_2(CO)_2(\mu\text{-}Cl)(\mu\text{-}CO)(dpm)_2^+$ with bromide or iodide in the bridgehead position, are synthesized by the addition of dpm under a CO atmosphere to an acetone-methanol solution containing $[Rh(CO)_2X_2]^-$ (X = Br^-, I^-), forming $[Rh_2(CO)_2(\mu\text{-}X)(\mu\text{-}CO)(dpm)_2]X$. Like the chloride analogue, the bromide-bridged complex loses its bridging CO when flushed with N_2 to form the complex, $Rh_2(CO)_2(Br)_2(dpm)_2$, however this reaction is much slower compared to the less stable species, $[Rh_2(CO)_2(\mu\text{-}Cl)(\mu\text{-}CO)(dpm)_2]Cl$.[9] In fact, by increasing the size of the bridging halide to iodide, the barrier to CO evolution is increased so much that the stable species, $[Rh_2(CO)_2(\mu\text{-}I)(\mu\text{-}CO)(dpm)_2]I$, remains intact. This has been explained in terms of steric interactions. The terminal carbonyl ligands in the complex, $[Rh_2(CO)_2(\mu\text{-}Cl)(\mu\text{-}CO)(dpm)_2]BPh_4$ have been shown by X-ray analysis to be bent away from the bridging chloride minimizing the non-bonded contacts. Therefore, as the size of halide increases the site adjacent to it becomes so crowded that the formation of the proposed intermediate (below) is inhibited.[9]



The yellow cationic A-frame complex, $[Rh_2(CO)_2(\mu\text{-}Cl)(dpm)_2]BPh_4$, is used extensively as a starting material for many other A-frame, double A-frame, and face-to-face dimers. No evidence exists for a Rh-Rh bond since this species has a Rh---Rh separation of 3.1521 Å, an acute angle of 82.38° (Rh-Cl-Rh), an average intraligand P---P separation of 3.092 Å, is diamagnetic, and has a "proximity-shifted" band at 445 nm in the electronic spectrum.[7,10]

The "proximity-shifted" band at 445 nm (λ_{max}) observed in the A-frame complex, $[Rh_2(CO)_2(\mu\text{-}Cl)(dpm)_2]BPh_4$, results from the electronic transition σ^* $(4d_{z2}) \rightarrow \sigma(5p_z)$. This metal-centered low energy absorption band is also observed in the face-to-face complexes, $Rh_2Cl_2(CO)_2(L\text{-}L)_2$, (L-L = dpm, dam), and $Rh_2(CNR)_4(L\text{-}L)_2$, (L-L =

dpm, dam). Since the ligand arrangement around each Rh atom, in $[Rh_2(CO)_2(\mu\text{-}Cl)(dpm)_2]BPh_4$, is approximately square planar, its molecular orbital scheme is assumed to be very similar to the face-to-face complexes which have no metal-metal bond. Contrary to this, the low-energy absorption bands of Rh(I) dimers having a metal-metal bond (e.g., $[Rh_2(CO)_2(\mu\text{-}Cl)(\mu\text{-}CO)(dpm)_2]BPh_4$, λ_{max} = 373 nm) are significantly blue-shifted.[11,12,13]

The addition of 1 equiv of isocyanide to the A-frame, $[Rh_2(CO)_2(\mu\text{-}Cl)(dpm)_2]BPh_4$, results in the formation of an unsymmetrical double A-frame complex, $[Rh_2(CO)(t\text{-}BuNC)(\mu\text{-}Cl)(\mu\text{-}CO)(dpm)_2]BPh_4$. The isocyanide attacks the $Rh_2(CO)_2(\mu\text{-}Cl)(dpm)_2^+$ at the terminal position between the bridging chloride and the terminal carbonyl ligand followed by rearrangement of the latter into a bridging position. This represents further proof for the bridge-terminal exchange mechanism occurring in the formation of $[Rh_2(CO)_2(\mu\text{-}Cl)(\mu\text{-}CO)(dpm)_2]BPh_4$ from $[Rh_2(CO)_2(\mu\text{-}Cl)(dpm)_2]BPh_4$. This compound also loses its CO in solution when bubbled with N_2 to yield a complex with a stretching frequency characteristic of an isocyanide, and one characteristic of a terminal CO, suggesting that the species is $[Rh_2(CO)(t\text{-}BuNC)(\mu\text{-}Cl)(dpm)_2]BPh_4$.[12]

The addition of 2 equiv and 4 equiv of isocyanide to $[Rh_2(CO)_2(\mu\text{-}Cl)(dpm)_2]BPh_4$ results in the formation of two symmetrical complexes, $[Rh_2(t\text{-}BuNC)_2(\mu\text{-}Cl)(\mu\text{-}CO)]BPh_4$ and $[Rh_2(t\text{-}BuNC)_4(dpm)_2](BPh_4)_2$, respectively. The latter complex readily reacts with CO and SO_2 to form the corresponding bridged

adducts, $[Rh_2(t\text{-}BuNC)_4(\mu\text{-}X)(dpm)_2]BPh_4$ (X = CO, SO_2). Both of these complexes display a symmetrical $^{31}P\ \{^1H\}$ NMR pattern indicative of the familiar AA'A"A'"XX' spin system.[12]

Another A-frame complex capable of reversibly binding carbon monoxide in the bridging position, and rapidly exchanging carbon monoxide, is the bridged bidentate acetate species, $[Rh_2(CO)_2(\mu\text{-}OOCCH_3)(dpm)_2]PF_6$. This cationic species is prepared by reacting silver acetate with $[Rh_2(CO)_2(\mu\text{-}Cl)(dpm)_2]PF_6$.[14]

The ^{13}CO enriched derivative of this complex has been shown by $^{13}C\ \{^1H\}$ NMR to rapidly exchange carbon monoxide at 30°C. Upon lowering the temperature to -70°C in the presence of excess CO a species having a symmetrical $^{31}P\ \{^1H\}$ NMR spectrum with the usual AA'A"A'"XX' pattern can be isolated. Its $^{31}P\ \{^1H\}$ NMR parameters ($\delta(P)$ = 30.0 ppm and $|^1J_{Rh\text{-}P} + {}^xJ_{Rh'\text{-}P}|$ = 93.2 Hz, relative to external 85% H_3PO_4) closely parallel those found for the double A-frame complex, $(Rh_2(CO)_2(\mu\text{-}CO)(\mu\text{-}Cl)(dpm)_2]BPh_4$ ($\delta(P)$ = 25.5 ppm and $|^1J_{Rh\text{-}P} + {}^xJ_{Rh'\text{-}P}|$ = 94.2 Hz. The further observation that the complex evolves CO upon warming and reverts to the starting material leads to the formulation of the species as $[Rh_2(CO)_2(\mu\text{-}CO)(\mu\text{-}OOCCH_3)(dpm)_2]PF_6$.[14]

The difference in stability between $[Rh_2(CO)_2(\mu\text{-}Cl)(\mu\text{-}CO)(dpm)_2]$-$PF_6$ and $[Rh_2(CO)_2(\mu\text{-}OOCCH_3)(\mu\text{-}CO)(dpm)_2]PF_6$ can be attributed to electronic and steric factors. The greater sigma donor strength of the chloride ligand relative to the acetate ligand tends to increase the electron density on the Rh atoms, thereby stabilizing the bridging carbonyl ligand through backbonding. The greater metal-metal

separation expected for the acetate could also contribute to the decreased stability of the bridging CO in the acetate complex.[14]

If an acetone solution of $[Rh_2(CO)_2(\mu\text{-}Cl)(\mu\text{-}SO_2)(dpm)_2]PF_6$ is bubbled with SO_2 for an excessive length of time, a disproportionation reaction occurs generating a brown precipitate, $Rh_2Cl_2(\mu\text{-}SO_2)(dpm)_2$, as one of the products. An X-ray analysis on this neutral complex showed it to have a distorted trigonal bipyramidal arrangement of ligands (including the other Rh) around each Rh atom, with a Rh-Rh distance of 2.784 Å being well within the range expected for a Rh-Rh single bond (2.617-2.797 Å). A metal-metal bond is further supported by the fact that the intraligand P---P distances are much larger than the Rh-Rh separation (P---P, 3.015 Å (avg.) compared to Rh-Rh, 2.784 Å). Also an acute Rh-S-Rh angle of 79.9° indicates significant contraction along the Rh-Rh axis. The complex is also diamagnetic, further substantiating a stable 16-electron system.[8]

The availability of the active site toward substrate binding depends largely on the coordinating ligands present in the A-frame complex. In $Rh_2Cl_2(\mu\text{-}SO_2)(dpm)_2$, the active site is effectively blocked by two endo-phenyl rings on the dpm ligands. This makes it difficult for an approaching substrate to bind in the active site.[8] This is a result of the severe twist about the Rh-Rh axis which acts to move the phenyl rings closer to the active site (P-Rh-Rh-P torsion angles are 6.32° and 7.61°). Although the active site is blocked by the endo-phenyl rings, the terminal sites adjacent to

the bridging SO_2 ligand are open to attack. Bubbling a solution of $Rh_2Cl_2(\mu\text{-}SO_2)(dpm)_2$ with CO results in the formation of the double A-frame complex, $Rh_2(CO)_2(\mu\text{-}Cl)(\mu\text{-}SO_2)(dpm)_2^+$. The attack of CO on $Rh_2Cl_2(\mu\text{-}SO_2)(dpm)_2$ is believed to occur at a terminal site, implying that these sites are vacant and open to attack.[10,15]

Although it was originally thought that two of the endophenyl rings (belonging to the dpm ligands) were effectively blocking the active site in $Rh_2(CO)_2(\mu\text{-}S)(dpm)_2$,[2] reaction with SO_2 yields the neutral double A-frame complex, $Rh_2(CO)_2(\mu\text{-}S)(\mu\text{-}SO_2)(dpm)_2$. This reversible reaction proceeds by the direct attack of SO_2 into the active site with no evidence of an intermediate species. In contrast to the complex, $[Rh_2(CO)_2(\mu\text{-}Cl)(dpm)_2]PF_6$,[12] $Rh_2(CO)_2(\mu\text{-}S)(dpm)_2$ (including its sulfur alkylated derivatives) does not react with CO to produce stable complexes. Electronic factors affecting stability in solution rather than structural effects in the solid seem to be the reason why $Rh_2(CO)_2(\mu\text{-}S)(dpm)_2$ fails to react with CO to form a stable complex.[3]

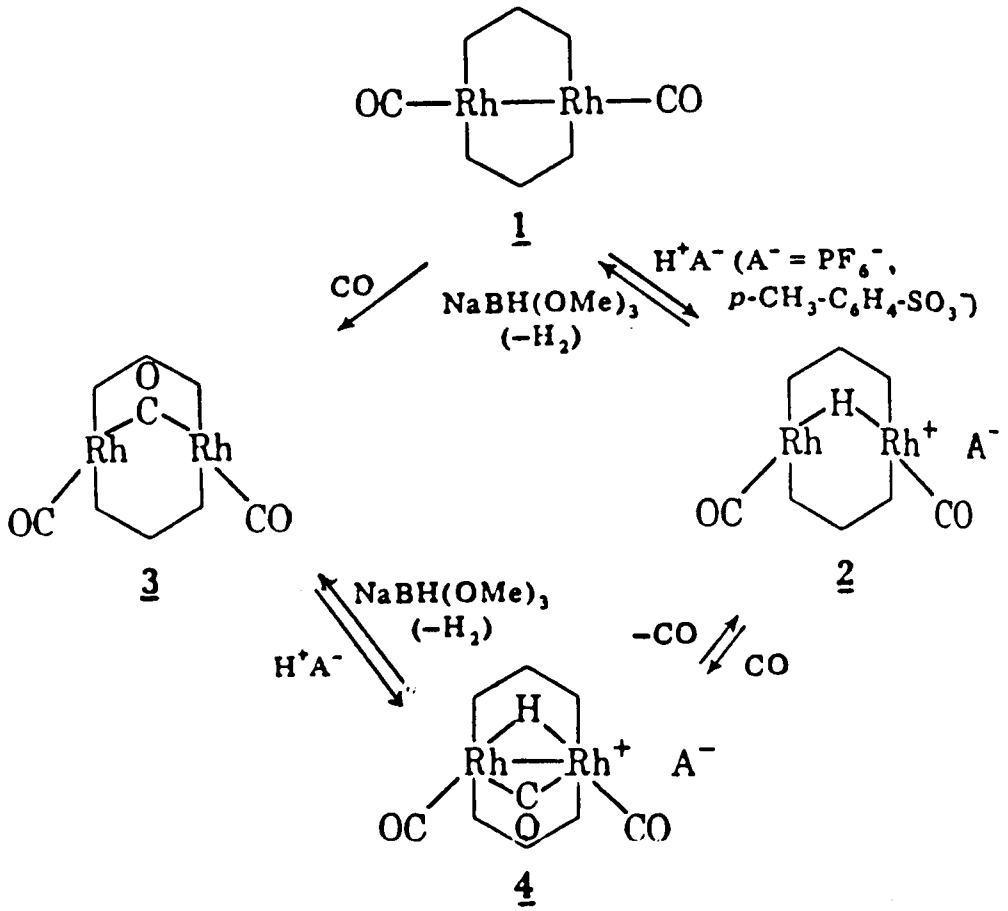
Side-by-side dimers possessing mutually <u>trans</u> dpm ligands are rarely reported in the literature since these coordinatively unsaturated complexes are so reactive. These complexes have a square planar geometry about each metal and are capable of forming some interesting A-frames by the direct insertion of small molecules into the metal-metal bond. An example of one of these, the Pd(I) dimer, $Pd_2X_2(dpm)_2$ (X = Cl, Br), was discussed earlier.[4]

In 1980 Eisenberg reported the first Rh(0) side-by-side dimer which is so highly reactive it has yet to be positively characterized. By reducing an ethanolic solution of $Rh_2Cl_2(CO)_2(dpm)_2$ with $NaBH_4$, a purple complex immediately precipitates from solution. Using spectroscopic and chemical evidence, including a single terminal carbonyl stretch of 1915 cm^{-1} in the infrared, this species was formulated as $Rh_2(CO)_2(dpm)_2$.[16]

Treatment of this dimer with either carbon monoxide or a large noncoordinating acid yields new dimers capable of reversibly binding CO or hydride in the bridging position. Some of the chemistry of $Rh_2(CO)_2(dpm)_2$ is shown below in Scheme I.[16]

The species $Rh_2(CO)_2(\mu\text{-}CO)(dpm)_2$ formed by the carbonylation of $Rh_2(CO)_2(dpm)_2$ was originally thought by Eisenberg to be an A-frame complex, but further evidence,[17] including a crystal structure analysis and ^1H NMR studies, indicated that the complex is a stereochemically nonrigid metal-metal bonded complex.[16] This fluxional complex has a coordination number of four around one Rh atom and a coordination number of five around the other Rh. The square planar arrangement around the Rh atom with coordination number four consists of two trans P donors (from the dpm ligands), a terminal CO, and the other Rh atom. The environment around the Rh atom with coordination number five is that of a distorted trigonal bipyramid, and consists of two cis P donors, a terminal carbon monoxide, the other Rh atom, and a bridging CO. The quasi-shared bridging CO in this complex is best viewed as a semibridging unsymmetrically

Scheme I


OC—Rh—Rh—CO
1
CO
NaBH(OMe)3
(–H2)
H+A– (A– = PF6–,
p-CH3-C6H4-SO3–)
O
C
Rh
Rh
OC
CO
3
H
Rh
Rh+
A–
OC
CO
2
NaBH(OMe)3
(–H2)
H+A–
–CO
CO
H
Rh—Rh+
A–
C
O
OC
CO
4

coordinated carbon monoxide skewed toward the Rh atom of coordination number five. The distances of the two Rh atoms to the bridging carbon are 2.533 Å and 1.857 Å.[17]

The intense purple complex, $[Rh_2(CO)_2(\mu\text{-}CO)(\mu\text{-}H)(dpm)_2]A$ ($A^- = PF_6^-$, $p\text{-}CH_2\text{-}C_6H_4\text{-}SO_3^-$), formed by one of two possible routes (see Scheme I) is analogous to $[Rh_2(CO)_2(\mu\text{-}CO)(\mu\text{-}Cl)(dpm)_2]PF_6$ in both its structure and some of its chemistry. The Rh-Rh separation of 2.732 Å, in addition to other structural parameters, supports the presence of a Rh-Rh single bond.[16]

An interesting reaction involving $[Rh_2(CO)_2(\mu\text{-}CO)(\mu\text{-}H)(dpm)_2]A$ was recently observed by Eisenberg.[18] When CO_2 is bubbled through a solution of $[Rh_2(CO)_2(\mu\text{-}CO)(\mu\text{-}H)(dpm)_2]A$, carbon monoxide is evolved with the concomitant production of a formate species, $[Rh_2(CO)_2(\mu\text{-}O_2CH)(dpm)_2]A$. This reaction occurs through the direct insertion of CO_2 into Rh-H-Rh and is reversible in the presence of CO. Another feature of the complex, $[Rh_2(CO)_2(\mu\text{-}CO)(\mu\text{-}H)(dpm)_2]A$, is that it is one of the most active catalysts in the water-gas shift reaction ($H_2O + CO \rightleftarrows CO_2 + H_2$), having a catalytic rate of 2.5 turnovers/hour.[18]

Another catalytic system of interest involves the parent species, $Rh_2(CO)_2(dpm)_2$, which reacts with acetylene or phenylacetylene to yield the corresponding bridged acetylene complexes. Both of these bridged species readily react with hydrogen to form the reduction products ethane or phenylethane.[16]

Extensive work on the chemistry of the face-to-face dimer, trans-$Rh_2Cl_2(CO)_2(dpm)_2$, with various halides was done by Cowie and his coworkers in 1980.[19] The asymmetrical bromo species, $[Rh_2Br(CO)(\mu\text{-}CO)(dpm)_2]Br$, is formed when an excess of NaBr is added to a solution of trans-$Rh_2Cl_2(CO)_2(dpm)_2$. This species has terminal and bridging carbonyl stretching frequencies of 1958 (s) and 1800 (m) cm^{-1}, respectively, along with an unsymmetrical $^{31}P\{^1H\}$ NMR spectrum. Upon sitting for several hours the terminal CO is evolved and the coordination of bromide occurs to yield the symmetric species, $Rh_2Br_2(\mu\text{-}CO)(dpm)_2$.

A similar reaction occurs when KI reacts with trans-$Rh_2Cl_2(CO)_2(dpm)_2$. It also has carbonyl bands in the bridging and terminal IR regions (1955 (s) and 1810 (m) cm^{-1}), in addition to an asymmetric $^{31}P\{^1H\}$ NMR spectrum. This species, $[Rh_2I(CO)(\mu\text{-}CO)(dpm)_2]I$, however, is stable and does not lose its terminal CO.[19] Steric factors are again responsible for the behavior of these halogen species. As the size of the halide increases the barrier to its recoordination also increases and the tendency to lose the terminal CO decreases.[19]

Reacting the unsymmetrical bromo and iodo species, $[Rh_2Br(CO)(\mu\text{-}CO)(dpm)_2]Br$ and $[Rh_2I(CO)(\mu\text{-}CO)(dpm)_2]I$, with CO or SO_2 yields double A-frame complexes with the familiar structure, $[Rh_2(CO)_2(\mu\text{-}X)(\mu\text{-}Y)(dpm)_2]X$ (X = Br, I; Y = CO, SO_2). The tricarbonyl species, $[Rh_2(CO)_2(\mu\text{-}X)(\mu\text{-}CO)(dpm)_2]X$ (X = Cl, Br), can

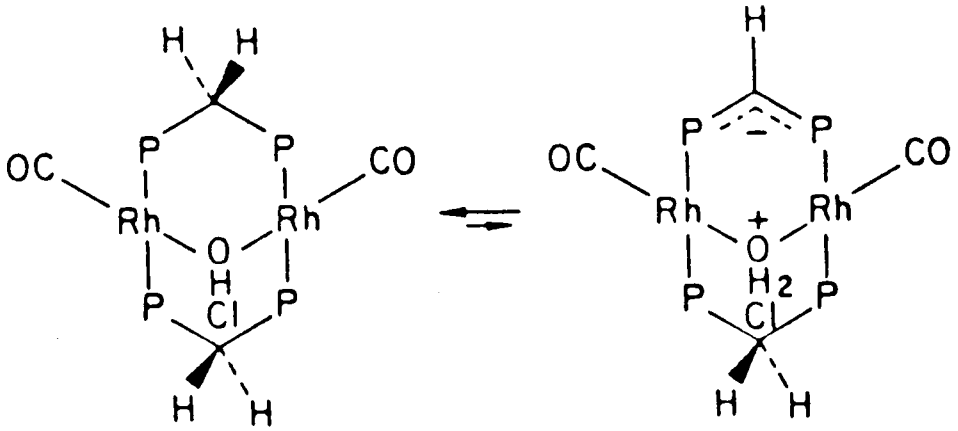
also be synthesized by bubbling carbon monoxide through a solution of either $Rh_2Cl_2(\mu\text{-}CO)(dpm)_2$ or $Rh_2Br_2(\mu\text{-}CO)(dpm)_2$.[19]

Prolonged bubbling of a solution containing, $[Rh_2(CO)_2(\mu\text{-}Br)(\mu\text{-}SO_2)(dpm)_2]Br$ or $[Rh_2(CO)_2(\mu\text{-}Cl)(\mu\text{-}SO_2)(dpm)_2]Cl$ with SO_2 yields the symmetric species, $Rh_2Br_2(\mu\text{-}SO_2)(dpm)_2$ and $Rh_2Cl_2(\mu\text{-}SO_2)(dpm)_2$, respectively. In contrast, the analogous stable iodo species, $[Rh_2(CO)_2(\mu\text{-}I)(\mu\text{-}SO_2)(dpm)_2]I$, fails to react with SO_2. With a few exceptions, symmetric complexes seem to be the rule rather than the exception with these Rh(I) dimers.[19]

A-frame complexes having an alkoxide ligand in the bridgehead position have recently been synthesized by treating either sodium methoxide or sodium ethoxide with an alcoholic suspension of <u>trans</u>-$Rh_2Cl_2(CO)_2(dpm)_2$ followed by the addition of excess $NaClO_4$. The products which precipitate from solution, $[Rh_2(CO)_2(\mu\text{-}X)(dpm)_2]ClO_4$ ($X = OCH_3$, OC_2H_5), each exhibit two terminal carbonyl stretching frequencies and feature the characteristic AA'A"A'"XX' pattern in the $^{31}P\ \{^1H\}$ NMR indicating that all four of the phosphorus atoms are chemically equivalent, but not magnetically equivalent. Both of these complexes undergo facile hydrolysis when H_2O is added forming the A-frame, $[Rh_2(CO)_2(\mu\text{-}OH)(dpm)_2]ClO_4$.[20]

A neutral A-frame complex having a chloride ligand hydrogen bonded to a bridging hydroxide ligand is prepared by adding $Na_2CO_3 \cdot 10H_2O$ to an alcoholic suspension of <u>trans</u>-$Rh_2Cl_2(CO)_2(dpm)_2$. Utilizing infrared, $^{31}P\ \{^1H\}$ NMR, and ^1H NMR, this complex has been

characterized as $[Rh_2(CO)_2(\mu\text{-}OH\text{---}Cl)(dpm)_2]\cdot H_2O$. The bridging group, $OH\text{---}Cl^{--}$, is extremely basic undergoing proton exchange with the dpm methylene protons in the presence of H_2O, albeit slowly. The exchange process has been followed by using D_2O and it is thought to proceed by the abstraction of a methylene proton by the bridging group, $OH\text{---}Cl^{--}$, followed by deuterium exchange both at the bridging OHCl and OH_2Cl groups and direct attack of D_2O on the bis(diphenylphosphino)methanide ligand as shown below.[20]

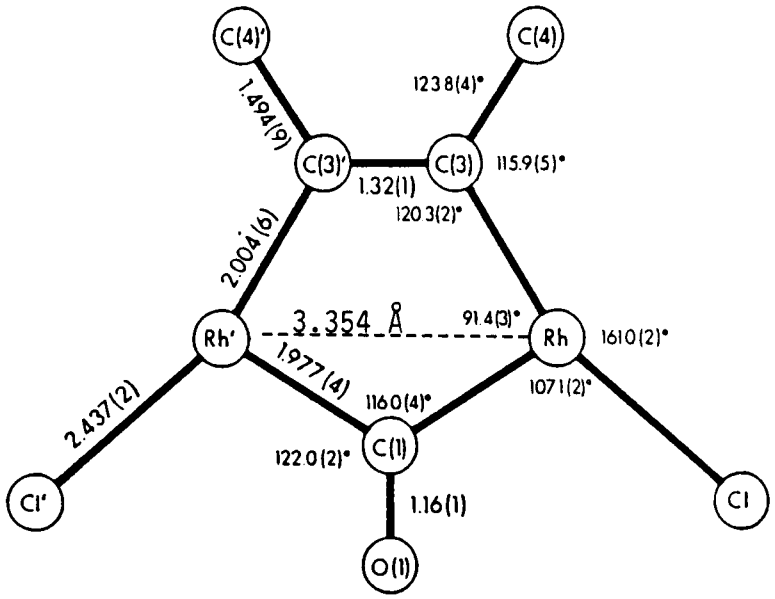


A-frame complexes having a pseudohalide ligand (NCO^-, SCN^-, N_3^-) in the bridging position can easily be prepared by the addition of KCNO, NH_4NCS, or NaN_3 to an acetone solution of $[Rh_2(CO)_2(\mu\text{-}O_2CCF_3)(dpm)_2]ClO_4$ forming the corresponding products, $[Rh_2(CO)_2(\mu\text{-}X)(dpm)_2ClO_4$ ($X = NCO^-$, NCS^-, N_3^-). All of these bridging N-bound products have virtually identical terminal carbonyl

stretching frequencies whose values are slightly higher than the corresponding bridged chloro or bromo analogues. This is a consequence of the greater sigma donor strength of the analogous chloro or bromo complexes which tends to increase the electron density on the metals decreasing the stretching frequency of the carbonyl ligands. Although bridging N-bound complexes of this type are relatively rare in rhodium complexes, confirmation for this N-bond formulation is supported by IR bands at 2196 cm^{-1} for the bridged NCO^- species, and two weak bands at 872 and 842 cm^{-1} for the bridged NCS^- species, all of which lie in the range normally seen for bridged N-bound complexes.[20]

In 1980 Cowie introduced a couple of stable Rh(I) double A-frame complexes having both ketonic carbonyl ligands (a bridging carbonyl ligand with no accompanying metal-metal bond) and bridging cis-dimetallated olefins.[21] These hitherto unknown dimers are synthesized by the reaction of DMA (dimethylacetylenedicarboyxlate) and HFB (hexafluoro-2-butyne) with either trans-$RH_2Cl_2(CO)_2(dpm)_2$ or $Rh_2Cl_2(\mu\text{-}CO)(dpm)_2$ yielding $Rh_2Cl_2(\mu\text{-}CO)(\mu\text{-}DMA)(dpm)_2$ and $Rh_2Cl_2(\mu\text{-}CO)(\mu\text{-}HFB)(dpm)_2$, respectively. The green $Rh_2Cl_2(\mu\text{-}CO)(\mu\text{-}DMA)(dpm)_2$ and its bridged HFB analogue have rather low carbonyl stretching frequencies of 1700 and 1705 cm^{-1}, respectively, well within the range of carbonyl frequencies for organic compounds. An X-ray crystal structure analysis on $Rh_2Cl_2(\mu\text{-}CO)(\mu\text{-}DMA)(dpm)_2$ gave the largest Rh---Rh separation presently known for a dimer containing a bridging carbonyl ligand

(3.354 Å). Below is a figure of the approximately planar metal-equatorial ligand framework for a dimetallated olefin complex.



Even with the long Rh---Rh separation, these complexes are unusually stable. Only prolonged refluxing (24 hours) of a solution containing $Rh_2Cl_2(\mu\text{-}CO)(\mu\text{-}HFB)(dpm)_2$ and a large excess of trimethylamine oxide rids the species of its ketonic carbonyl ligand to form $Rh_2Cl_2(\mu\text{-}HFB)(dpm)_2$.[21]

A crystal structure of $Rh_2Cl_2(\mu\text{-}HFB)(dpm)_2$ indicates the presence of a metal-metal bond with a Rh-Rh distance of 2.745 Å and a bridging acetylene ligand coordinated as a cis-dimetallated olefin. The complex has approximately C_{2v} symmetry with a distorted trigonal bipyramidal arrangement of ligands around each Rh atom. The structural parameters are typical of most other A-frames (Rh-P distances range from 2.309-2.346 Å).[22]

Reactions with carbon monoxide indicate a direct attack at the active site to form $Rh_2Cl_2(\mu\text{-}CO)(\mu\text{-}HFB)(dpm)_2$. The CF_3 groups contained in the HFB ligand facilitate the direct attack of CO at the bridged position since these groups are effectively blocking the terminal positions.[22]

Acetylene bridged complexes of the form, $[Rh_2(CO)(OOCCH_3)(\mu\text{-}CO)(\mu\text{-}X)(dpm)_2]PF_6$ (X = HFB, DMA) are produced upon reaction of $[Rh_2(CO)_2(\mu\text{-}OOCCH_3)(dpm)_2]PF_6$ with HFB or DMA. Further reaction of these unsymmetrical complexes with 1.5 equiv of tert-butyl isocyanide or trimethylphosphite leads to dissociation of the terminal CO forming the products, $[Rh_2Y(OOCCH_3)(\mu\text{-}CO)(\mu\text{-}X)(dpm)_2]PF_6$ (X = HFB, DMA; Y = $P(OMe)_3$, $CNBu^t$). These complexes all feature an asymmetrical $^{31}P\{^1H\}$ NMR spectrum with an AA'BB'XY pattern. X-ray analysis and conventional electron counting support a ketonic carbonyl ligand formulation for these complexes. Substituting the terminal carbonyl ligand in $[Rh_2(CO)(OOCCH_3)(\mu\text{-}CO)(\mu\text{-}X)(dpm)_2]PF_6$ (X = HFB, DMA), with either tert-butyl isocyanide or trimethylphosphite leads to a pronounced lowering of the stretching frequency for the bridging carbonyl ligand from 1752 (m) cm^{-1} for the $[Rh_2(CO)(OOCCH_3)(\mu\text{-}CO)(\mu\text{-}HFB)(dpm)_2]PF_6$, to 1715 (s) cm^{-1} for the $[Rh_2(P(OCH_3)_3)(OOCCH_3)(\mu\text{-}CO)(\mu\text{-}HFB)(dpm)_2]PF_6$.[14]

B. Statement of Purpose

This work investigates the spectroscopic and electrochemical properties of new dinuclear Rh(I) A-frame complexes, and their halogenated Rh(II) derivatives, in which the triazolate anion and pyrazolate derivatives are incorporated as bridgehead ligands. Since little is known about dinuclear Rh(I) A-frame complexes having an N N' bidentate ligand bridging the two metals, it was of interest to study the properties of this class of complexes. Since it has been shown that rhodium(I) dimers undergo oxidative-addition reactions,[23-25] it was also of interest to study this class of reactions, particularly the oxidative addition by I_2, Br_2, or Cl_2 to the pyrazolate or triazolate complexes.

Very few Rh(II) dimers with bridging dpm (bis(diphenylphosphino)methane) ligands have been investigated in recent years. Among the Rh(II) complexes that have been investigated are the tetrakis(carboxylato) complexes, and complexes formed by substitution of the carboxylato with other anionic bidentate ligands.[26-28]

In recent years electrochemical studies have been done on tetrakis(isocyanide)rhodium(I) complexes in the presence of nitrogenous bases.[29,30] In these studies it was found that tetrakis-(isocyanide)rhodium(I) complexes were more easily oxidized in the presence of a coordinating species. It was also shown that in the presence of pyridine and some substituted pyridines, a direct correlation exists between the basicity of nitrogenous ligands and the

ease with which these tetrakis(isocyanide)Rh(I) complexes can be oxidized.

Since rhodium complexes, with bridging dpm and dam(bis-(diphenyl)arsinomethane) ligands, have been synthesized electrochemically in the presence of coordinating ligands, it was of interest to use this method and characterize other novel rhodium complexes.

CHAPTER II

EXPERIMENTAL

A. Chemicals

1. Solvents

a. Methylene chloride (CH_2Cl_2). Certified ACS Spectro-analyzed (Fisher Scientific) was used without further purification.

b. Benzene. Certified ACS benzene (Fisher Scientific) was used without further purification.

c. Acetone. Certified ACS acetone (Fisher Scientific) was used without further purification.

d. Methanol. Certified ACS methanol (Fisher Scientific) was used without further purification.

e. Ethanol. Certified ethanol (Aaper) was used without further purification.

f. Diethyl ether (ether). Certified ACS anhydrous ether (Fisher Scientific) was used without further purification.

g. Ligroin. Certified ACS 30-60 ligroin (Fisher Scientific) was used without further purification.

h. Chloroform. Certified ACS chloroform (Fisher Scientific) was used without further purification.

i. Toluene. Certified ACS toluene (Fisher Scientific) was used without further purification.

j. Tetrahydrofuran (THF). Certified ACS THF (Fisher Scientific) was distilled over Na/benzophenone (Fisher Scientific, Certified ACS) immediately before its use.

k. Distilled water (water). Departmental distilled water was used without further purification.

l. 1,2-Dichloroethane. Certified ACS (Fisher Scientific) was used without further purification.

2. Reagents

a. Tetrabutylammonium iodide (TBAI). Reagent grade TBAI (Aldrich) was used without further purification.

b. Potassium hexafluorophosphate (KPF_6). Reagent grade KPF_6 (Alpha) was used without further purification.

c. Bis(diphenylphosphino)methane (dpm). Reagent grade dpm (Strem) was used without further purification.

d. Tetrabutylammonium chloride (TBAC). Reagent grade TBAC (Strem) was recrystallized five times from acetone-ether, then dried in vacuo at ca. 55°C.

e. Tetrabutylammonium hexafluorophosphate (TBAH). TBAH was prepared by metathesis of TBAI and KPF_6 in water, then recrystallized five times from acetone-water.

f. Rhodium(III) chloride trihydrate ($RhCl_3 \cdot 3H_2O$). Reagent grade $RhCl_3 \cdot 3H_2O$ (Strem and Johnson Matthey) was used without further purification.

g. Phosphorus pentoxide (P_2O_5). Certified ACS P_2O_5 (Fisher Scientific) was used without further purification.

h. Rhodium(I) dichlorotetracarbonyl ($Rh_2Cl_2(CO)_4$). $Rh_2Cl_2(CO)_4$ is prepared by bubbling ethanol enriched CO through $RhCl_3 \cdot 3H_2O$ (contained in a glass frit) at 100°C for two hours. The red solid is sublimed at 100°C and placed in the dessicator.

3. Miscellaneous

a. Argon (Ar). Prepurified Ar (Burdett, MG Industries) was used without further purification.

b. Nitrogen (N_2). Prepurified N_2 (MG Industries) was used without further purification.

c. Carbon monoxide (CO). Prepurified CO (Matheson) was used without further purification.

d. Chlorine (Cl_2). Cl_2 was prepared by introducing 5 mL of HCl (62.0 mmole) into a flask containing 1.22 g of $KMnO_4$ (7.75 mmole). The Cl_2 was then bubbled through concentrated H_2SO_4 (200 mL) before reacting with the appropriate complex. Residual Cl_2 was neutralized by bubbling it into 6 M NaOH.

e. Nujol. Nujol (Plough, Inc.) was used after drying over Na.

f. Hydrochloric acid (HCl). Certified ACS HCl (Fisher Scientific) was used without further purification.

g. Potassium permanganate ($KMnO_4$). Certified ACS $KMnO_4$ (Fisher Scientific) was used without further purification.

h. Sulfuric acid (H_2SO_4). Certified ACS H_2SO_4 (Fisher Scientific) was used without further purification.

i. Sodium hydroxide (NaOH). Certified NF NaOH (Fisher Scientific) was used without further purification.

j. n-Butyllithium ($\underline{n}$-C_4H_9Li). Reagent grade 2.5 M $\underline{n}$-C_4H_9Li in hexanes (Aldrich) was used without further purification.

k. Bromine (Br_2). Certified ACS Br_2 (Fisher Scientific) was used without further purification.

l. Tetrabutylammonium nitrate (TBAN). Reagent grade TBAN (Fluka AG) was recrystallized three times from chloroform-ligroin and dried for 24 hours in vacuo at 50°C.

m. 3,5-Dimethylpyrazole (3,5-DMP). Reagent grade 3,5-DMP (Aldrich) was used without further purification.

n. Pyrazole (Pz). Reagent grade Pz (Aldrich) was used without further purification.

o. 4-Methylpyrazole (4-MP). Reagent grade 4-MP (Aldrich) was used without further purification.

p. 1,2,4-Triazole (Triaz). Reagent grade Triaz (Aldrich) was used without further purification.

q. 4-Bromo-3,5-dimethylpyrazole (4B-3,5-DMP). Reagent grade 4B-3,5-DMP (Pfaltz and Bauer) was used without further purification.

r. Iodine (I_2). Reagent grade I_2 (Fisher Scientific) was used without further purification.

B. Spectroscopy

1. Infrared Spectroscopy

Infrared spectra were recorded on a Digilab FTS-20 C/V Fourier Transform Infrared Spectrometer or a Perkin-Elmer 1330 Infrared Spectrophotometer. Solid samples were prepared as Nujol mulls sealed between thin polyethylene sheets.

2. Ultraviolet-Visible Spectroscopy

Ultraviolet-visible spectra were recorded on a Cary 219 Spectrophotometer. Quartz cells (Fisher Scientific) of 1.0 cm pathlength were used. All solvents used to record UV-Vis spectra were of spectroscopic grade.

3. Nuclear Magnetic Resonance Spectroscopy (NMR)

$^{31}P\ \{^1H\}$-NMR spectra were recorded on a JEOL FX 90Q Fourier Transform NMR Spectrometer at 36.19 MHz using 85% H_3PO_4 (Fisher

Scientific) or trimethylphosphate (Aldrich) as the external reference. The spectrometer was locked on the deuterium signal of CD_2Cl_2, $CDCl_3$ or $(CD_3)_2CO$.

C. Electrochemistry

1. Bulk Electrolysis, Coulometry, and Cyclic Voltammetry

Bulk electrolysis, coulometry, and cyclic voltammetry were performed on either a BAS 100 Electrochemical Analyzer (Bioanalytical Systems, Inc.) coupled with a DMP-40 Series Digital Plotter (Houston Instrument) or a Model 363 Potentiostat/Galvanostat (EG&G Princeton Applied Research Company) coupled with a Digital Coulometer (Model 640, Electrosynthesis Company). The voltammograms obtained using the 363 Potentiostat/Galvanostat were recorded on an omnigraphic 2000 X-Y Recorder (Houston Instrument).

2. Electrodes

For bulk electrolysis and coulometry a three electrode system was used in which the working electrode was a 17.5 cm^2 platinum grid; the isolated counter electrode was a carbon rod; and the reference electrode which was separated from the bulk solution by a fine frit, was a saturated calomel electrode (SCE).

For cyclic voltammetry a 0.24 cm^2 platinum button electrode (Beckman) served as the working electrode; a 17.5 cm^2 platinum grid served as the counter electrode; and a SCE was used as the reference electrode.

3. Cells

For bulk electrolysis and coulometry an H-shaped, three-compartment cell was utilized in which the three compartments were separated by fine glass frits. The working electrode compartment was fitted with a glass frit bottom used for degassing and stirring the solution.

The cells used for cyclic voltammetry were either a one-compartment cell or an H-shaped, three-compartment cell when bulk electrolysis was also to be performed on the solution. The one-compartment cell was fitted with a glass frit and a side arm to degass the solution and maintain an inert atmosphere over the solution.

D. Elemental Analysis

Elemental analyses were performed by Galbraith Laboratories, Inc. of Knoxville, Tennessee or Schwarzkopf Microanalytical Laboratory of Woodside, New York.

E. Preparation of Rhodium Complexes

1. μ-Carbonyldicarbonyl-μ-chlorobis[μ-methylenebis[diphenylphosphine]-P:P']-dirhodium(I) Hexafluorophosphate, $[Rh_2(CO)_3Cl(dpm)_2][PF_6]$

The procedure that Mague and Sanger[7] used to make the analogous BPh_4^- complex was used to prepare 1. A red solution consisting of 0.200 g of $RhCl_3 \cdot 3H_2O$ in 25 mL of ethanol and 0.5 mL of water was refluxed for 5 hours while being bubbled with CO. The

resulting lemon yellow solution was allowed to cool to room temperature and solutions of 0.27 g dpm in 3 mL of acetone and 0.11 g ammonium hexafluorophosphate in 3 mL of ethanol were added in rapid succession while maintaining the flow of CO. After the evolution of CO, the product which was precipitated as yellow crystals was then filtered. After being washed with water, ethanol, and ether, the complex was dried in vacuo. The yield was 70%.

IR spectrum: ν(CO) in Nujol = 2003 cm^{-1} (sh), 1982 cm^{-1} (s) and 1875 cm^{-1} (m) (lit. 7 for BPh_4^- complex: 1992 cm^{-1}, 1953 cm^{-1}, and 1869 cm^{-1}).

2. Dicarbonyl-μ-chlorobis[μ-methylenebis[diphenylphosphine]-P:P']-dirhodium(I) Hexafluorophosphate, $[Rh_2(CO)_2Cl(dpm)_2][PF_6]$

The procedure that Mague and Sanger[7] used to make the analogous BPh_4^- complex was used to prepare 2. A yellow-orange solution of 1.2 g of 1 in 25 mL of acetone was bubbled with Ar for 20 minutes. The orange solution was treated with 1:1 ether-ligroin until the cloud point was reached. The bright yellow crystals were filtered, washed with ether, and dried in vacuo. The yield was 45%.

IR spectrum: ν(CO) in Nujol = 1994 cm^{-1} (sh) and 1978 cm^{-1} (s) (lit. for BPh_4^- complex: 1997 cm^{-1} and 1978 cm^{-1}).

3. trans-Dicarbonyldichlorobis[μ-methylenebis[diphenylphosphine]-P:P']-dirhodium(I), $Rh_2(CO)_2Cl_2(dpm)_2$

Method A of Mague and Mitchner[31] was used to prepare 3. To 0.40 g of $Rh_2(CO)_4Cl_2$ dissolved in 20 mL of benzene was added 1.6 g

of dpm dissolved in 20 mL of benzene. Ether was added to the cloud point and the solution was cooled at -10°C for 24 hours. The orange product was collected by filtration, washed with ether, and dried in vacuo. The yield was 90%.

IR spectrum: ν(CO) in Nujol = 1971 cm^{-1} (s) (lit. 31: 1976 cm^{-1} (s)).

4. μ-Carbonyl-μ-chlorodichlorobis[μ-methylenebis[diphenylphosphine]-P:P']-dirhodium(II) Hexafluorophosphate, $[Rh_2(CO)Cl_3(dpm)_2][PF_6]$

This complex was prepared by a procedure outlined by Tinsley.[32] A CH_2Cl_2 solution of 3 (141.4 mg, 0.128 mmol) which contained 0.1 M TBAH and TBAC (355.7 mg, 1.28 mmol) was oxidized at 0.70 V (vs SCE) via controlled potential electrolysis. The resulting reddish-brown solution was then reduced in volume (5 mL) and 50 mL of CH_3OH was added. The resultant green suspension was stirred for 24 hours, collected by filtration, washed with water, and dried in vacuo. The green solid was recrystallized from CH_2Cl_2, filtered, and dried in vacuo. Yield: 60%.

IR spectrum in Nujol: ν(CO) = 1799 cm^{-1} (s). The spectrum also shows PF_6^- peaks at 839 cm^{-1} (s) and 560 cm^{-1} (m). UV-Vis spectrum in CH_2Cl_2 [$\lambda_{max}(\varepsilon)$]: 365 nm (13,000), 315 nm (27,000). $^{31}P\{^1H\}$ NMR spectrum δ = 9.33 ppm (from 85% H_3PO_4), [^1J(Rh-P) + ^xJ(Rh-P)] = 97.66 Hz. Anal. calcd. for $C_{51}H_{44}Cl_3F_6OP_5Rh_2$: C, 48.85; H, 3.54; Cl, 8.48; P, 12.35. Found: C, 47.47; H, 3.80; Cl, 8.77; P, 11.67.

5. Trichloro-μ-chlorocarbonylbis[μ-methylenebis[diphenylphosphine]-[-P:P']-dirhodium(II), $[Rh_2Cl_4(CO)(dpm)_2]$

a. Method 1. A CH_2Cl_2 solution of 4 (154 mg, 0.123 mmol) was bubbled with CO for one hour. During the first few minutes of the reaction, the green solution turned brown to red to finally a yellow-orange color. The solution was reduced in volume (25 mL) and transferred to a 100 mL beaker. Slow diffusion of ether into the solution (few days) resulted in the formation of orange and black crystals. The orange crystals proved to be identical to 2.

b. Method 2. To a CH_2Cl_2 solution of 4 (105 mg, 0.087 mmol) was added excess TBAC. The brown solution was stirred for one hour, then reduced in volume to 5 mL and 50 mL of diethyl ether was added. The product was collected by filtration, washed with copious amounts of water and ether, then dried in vacuo.

IR spectrum: ν(CO) in Nujol = 2028 cm^{-1} (s). UV-Vis spectrum in CH_2Cl_2 [$\lambda_{max}(\varepsilon)$]: 383 nm (11,500), 303 nm (23,600). $^{31}P\{^1H\}$ NMR spectrum is an AA'BB'XY pattern, whose δ (P) and coupling constants can only be determined by NMR computer simulation. Anal. calcd. for $C_{51}H_{44}Cl_4OP_4Rh_2$: Cl, 12.39. Found: Cl, 11.18.

6. Dicarbonyl-μ-3,5-dimethylpyrazolatobis[μ-methylenebis[diphenylphosphine]-P:P']-dirhodium(I) Hexafluorophosphate, $[Rh_2(CO)_2(C_5H_7N_2)(dpm)_2][PF_6]$

This compound was made by dissolving $[Rh_2(CO)_2(\mu\text{-}Cl)(dpm)_2][PF_6]$ (297 mg, 0.245 mmol) and 3,5-dimethylpyrazole (248 mg, 0.258 mmol)

in separate flasks with freshly distilled THF. To the solution containing 3,5-dimethylpyrazole was added n-BuLi (0.10 mL, 0.250 mmol). Slow dropwise addition of this solution to the solution containing $[Rh_2(CO)_2(\mu\text{-}Cl)(dpm)_2][PF_6]$ resulted in a color change from yellow to dark orange to reddish orange and finally to red. The solution was stirred for 20 minutes. An orange solid precipitated after 10 minutes of stirring and the suspension was reduced in volume (10 mL) and 50 mL of diethyl ether was added. The solid was collected by filtration, recrystallized from CH_2Cl_2/diethyl ether, and dried in vacuo.

IR spectrum: ν(CO) in Nujol = 1975 cm^{-1} (s) and 1962 cm^{-1} (s). The spectrum also shows PF_6^- peaks at 839 cm^{-1} (s) and 560 cm^{-1} (m). UV-Vis spectrum in CH_2Cl_2 [$\lambda_{max}(\varepsilon)$]: 484 nm (20,500). $^{31}P\{^1H\}$ NMR spectrum: δ = 22.69 ppm (from 85% H_3PO_4), [^1J(Rh-P) + ^xJ(Rh-P)] = 129.4 Hz. Anal. calcd. for $C_{57}H_{51}F_6N_2O_2P_5Rh_2$: C, 53.88; H, 4.05. Found: C, 52.38; H, 4.20.

7. Dicarbonyl-μ-pyrazolatobis[μ-methylenebis[diphenylphosphine]-P:P']-dirhodium(I) Hexafluorophosphate, $[Rh_2(CO)_2(C_3H_3N_2)(dpm)_2][PF_6]$

Compound 7 was produced by the same procedure used to make 6. Using pyrazole (43.1 mg, 0.633 mmol), n-BuLi (0.425 mL, 0.658 mmol) and $[Rh_2(CO)_2(\mu\text{-}Cl)(dpm)_2][PF_6]$ (766.9 mg, 0.633 mmol), a deep red solid was obtained.

IR spectrum: ν(CO) in Nujol = 1988 cm^{-1} (s) and 1967 cm^{-1} (s). The spectrum also shows PF_6^- peaks at 839 cm^{-1} (s) and 560

cm^{-1} (m). UV-Vis spectrum in CH_2Cl_2 [$\lambda_{max}(\varepsilon)$]: 492 nm (15,200). $^{31}P\ \{^1H\}$ NMR spectrum: δ = 19.25 ppm (from 85% H_3PO_4), [^1J(Rh-P) + ^xJ(Rh-P)] = 128.9 Hz. Anal. calcd. for $C_{55}H_{47}F_6N_2O_2P_5Rh_2$: C, 53.16; H, 3.81; N, 2.25. Found: C, 51.93; H, 4.29; N, 2.03.

8. Dicarbonyl-μ-4-methylpyrazolatobis[μ-methylenebis[diphenylphosphine]-P:P']-dirhodium(I) Hexafluorophosphate, $[Rh_2(CO)_2(C_4H_5N_2)(dpm)_2][PF_6]$

Compound 8 was prepared by the same procedure used to make 6. Using 4-methylpyrazole (82.7 mL, 0.278 mmol), n-BuLi (0.111 mL, 0.278 mmol), and $[Rh_2(CO)_2(\mu\text{-}Cl)(dpm)_2][PF_6]$ (323 mg, 0.278 mmol) and orange-red solid was obtained.

IR spectrum: ν (CO) in Nujol = 1984 cm^{-1} (s) and 1973 cm^{-1} (s). The spectrum also shows PF_6^- peaks at 839 cm^{-1} (s) and 560 cm^{-1} (m). UV-Vis spectrum in CH_2Cl_2, [$\lambda_{max}(\varepsilon)$]: 493 nm (20,300). $^{31}P\ \{^1H\}$ NMR spectrum: δ = 24.44 ppm (from 85% H_3PO_4), [^1J(Rh-P) + ^xJ(Rh-P)] = 129.4 Hz. Anal. calcd. for $C_{56}H_{49}F_6N_2O_2P_5Rh_2$: C, 53.52; H, 3.93. Found: C, 52.03; H, 4.23.

9. Dicarbonyl-μ-triazolatobis[μ-methylenebis[diphenylphosphine]-P:P']-dirhodium(I) Hexafluorophosphate, $[Rh_2(CO)_2(C_2H_2N_3)(dpm)_2)][PF_6]$

Compound 9 was prepared by the same procedure used to make 6. Using triazole (68.0 mg, 0.984 mmol), n-BuLi (0.394 mL, 0.984 mmol), and $[Rh_2(CO)_2(\mu\text{-}Cl)(dpm)_2][PF_6]$ (1.139 g, 0.940 mmoles) an orange-red solid was obtained.

IR spectrum: ν (CO) in Nujol = 1991 cm^{-1} (s). The spectrum also shows PF_6^- peaks at 839 cm^{-1} (s) and 560 cm^{-1} (m). UV-Vis spectrum in CH_2Cl_2, [$\lambda_{max}(\varepsilon)$]: 487 nm (19,000). $^{31}P\ \{^1H\}$ NMR spectrum: δ = 23.47 ppm (from 85% H_3PO_4), [^1J(Rh-P) + ^xJ(Rh-P)] = 127.0 Hz. Anal. calcd. for $C_{55}H_{46}F_6N_3O_2P_5Rh_2$: C, 52.15; H, 3.73. Found: C, 51.80; H, 4.05.

10. Dicarbonyldiiodo-μ-3,5-dimethylpyrazolatobis[μ-methylenebis-[diphenylphosphine]-P:P']-dirhodium(II) Hexafluorophosphate, $[Rh_2(CO)_2I_2(C_5H_7N_2)(dpm)_2][PF_6]$

To a stirred CH_2Cl_2 solution of 6 (68.0 mg, 0.0535 mmol) solid I_2 (13.6 mg, 0.0623 mmol) was added. The red-brown solution was stirred for 20 minutes, then reduced in volume to 5 mL and 50 mL of diethyl ether was added. The product was collected by filtration, recrystallized from CH_2Cl_2/diethyl ether, and dried in vacuo.

IR spectrum: ν (CO) in Nujol = 2056 cm^{-1} (s). The spectrum also shows PF_6^- peaks at 839 cm^{-1} (s) and 560 cm^{-1} (m). UV-Vis spectrum in CH_2Cl_2, [$\lambda_{max}(\varepsilon)$]: 511 nm (15,000), 450 nm (19,400), 399 nm (21,600), 320 nm (19,700). $^{31}P\ \{^1H\}$ NMR spectrum: δ = 6.40 ppm (from 85% H_3PO_4), [^1J(Rh-P) + ^xJ(Rh-P)] = 85.4 Hz. Anal. calcd. for $C_{57}H_{51}F_6I_2N_2O_2P_5Rh_2$: C, 44.91; H, 3.37; I, 16.65. Found: C, 43.59; H, 3.48; I, 15.59.

11. Dicarbonyldiiodo-μ-pyrazolatobis[μ-methylenebis[diphenylphosphine]-P:P']-dirhodium(II) Hexafluorophosphate, $[Rh_2(CO)_2I_2(C_3H_3N_2)(dpm)_2][PF_6]$

Compound 17 was prepared by the same procedure used to make 16. Using 7 (252.7 mg, 0.203 mmol) and I_2 (51.6 mg, 0.203 mmol) a red-brown solid was obtained.

IR spectrum: ν (CO) in Nujol = 2065 cm^{-1} (s) and 2031 cm^{-1} (m). The spectrum also shows PF_6^- peaks at 839 cm^{-1} (s) and 560 cm^{-1} (m). UV-Vis spectrum in CH_2Cl_2, [$\lambda_{max}(\varepsilon)$]: 509 nm (13,600), 440 nm (18,700), 410 nm (19,400), 311 nm (17,300), 272 nm (30,600). $^{31}P\ \{^1H\}$ NMR spectrum: δ = 4.82 ppm (from 85% H_3PO_4), [^1J(Rh-P) + ^xJ(Rh-P)] = 83.0 Hz. Anal. calcd. for $C_{55}H_{47}F_6I_2N_2O_2P_5Rh_2$: C, 44.14; H, 3.17; I, 16.96. Found: C, 43.62; H, 3.29; I, 16.26.

12. Dicarbonyldiiodo-μ-4-methylpyrazolatobis[μ-methylenebis[diphenylphosphine]-P:P']-dirhodium(II) Hexafluorophosphate, $[Rh_2(CO)_2I_2(C_4H_5N_2)(dpm)_2][PF_6]$

Compound 18 was prepared by the same procedure used to make 16. Using 8 (47.8 mg, 0.038 mmol) and I_2 (9.6 mg, 0.038 mmol), a red-brown solid was obtained.

IR spectrum: ν (CO) in Nujol = 2063 cm^{-1} (s) and 2031 cm^{-1} (sh). The spectrum also shows PF_6^- peaks at 839 cm^{-1} (s) and 560 cm^{-1} (m). UV-Vis spectrum in CH_2Cl_2, [$\lambda_{max}(\varepsilon)$]: 508 nm (18,300), 436 nm (25,400), 411 nm (25,600), 343 nm (19,400). $^{31}P\ \{^1H\}$ NMR spectrum: δ = 4.89 ppm (from 85% H_3PO_4), [^1J(Rh-P) + ^xJ(Rh-P)] =

83.0 Hz. Anal. calcd. for $C_{56}H_{49}F_6I_2N_2O_2P_5Rh_2$: C, 44.53; H, 3.27; I, 16.80. Found: C, 42.89; H, 3.42; I, 17.03.

13. Dicarbonyldiiodo-μ-triazolatobis[μ-methylenebis[diphenylphosphine]-P:P']-dirhodium(II) Hexafluorophosphate, $[Rh_2(CO)_2I_2(C_2H_2N_3)(dpm)_2][PF_6]$

Compound 19 was prepared by the same procedure used to make 16. Using 9 (120.8 mg, 0.097 mmol) and I_2 (24.7 mg, 0.097 mmol), a red-brown solid was obtained.

IR spectrum: ν (CO) in Nujol = 2063 cm^{-1} (s) and 2031 cm^{-1} (s). The spectrum also shows PF_6^- peaks at 839 cm^{-1} (s) and 560 cm^{-1} (m). UV-Vis spectrum in CH_2Cl_2 [$\lambda_{max}(\varepsilon)$]: 511 nm (15,000), 443 nm (21,400), 406 nm (24,500), 293 nm (34,000). $^{31}P\{^1H\}$ NMR spectrum: δ = 5.29 ppm (from 85% H_3PO_4), [$^1J(Rh-P) + {}^xJ(Rh-P)$] = 83.0 Hz. Anal. calcd. for $C_{54}H_{46}F_6I_2N_3O_2P_5Rh_2$: C, 43.31; H, 3.10; I, 16.95. Found: C, 42.74; H, 3.15; I, 17.34.

14. Dibromodicarbonyl-μ-4-bromo-pyrazolatobis[μ-methylenebis[diphenylphosphine]-P:P']-dirhodium(II) Hexafluorophosphate, $[Rh_2Br_2(CO)_2(C_3H_2BrN_2)(dpm)_2][PF_6]$

Compound 24 was prepared by adding Br_2 (ℓ) (0.015 mL, 0.2912 mmol) to a stirred methylene chloride solution of 7 (360.4 mg, 0.290 mmol). The orange solution was stirred for 20 minutes, then reduced in volume (10 mL). Diethyl ether (50 mL) was added and the orange-yellow solid was collected by filtration, recrystallized from CH_2Cl_2/diethyl ether, and dried in vacuo.

IR spectrum: ν (CO) in Nujol = 2061 cm^{-1} (s) and 2033 cm^{-1} (sh). The spectrum also shows PF_6^- peaks at 839 cm^{-1} (s) and 560 cm^{-1} (m). UV-Vis spectrum in CH_2Cl_2 [$\lambda_{max}(\varepsilon)$]: 387 nm (20,700), 309 nm (22,500), 267 nm (28,900). $^{31}P\ \{^1H\}$ NMR spectrum: δ = 8.93 ppm (from 85% H_3PO_4), [^1J(Rh-P) + ^xJ(Rh-P)] = 80.6 Hz.

15. Dibromodicarbonyl-μ-4-bromo-3,5-dimethylpyrazolatobis[μ-methylenebis[diphenylphosphine]-P:P']-dirhodium(II) Hexafluorophosphate, $[Rh_2Br_2(CO)_2(C_5H_6BrN_2)(dpm)_2][PF_6]$

a. Method 1. Compound 25 was prepared by the same procedure used to make 24. Using Br_2 (ℓ) (0.011 mL, 0.214 mmol) and 6 (263.0 mg, 0.207 mmol) an orange solid was obtained.

b. Method 2. Compound 25 was prepared by the same procedure used to make 24. Using Br_2 (ℓ) (0.0187 mL, 0.363 mmol) and 10 (466.9 mg, 0.346 mmol) an orange solid was obtained.

IR spectrum: ν (CO) in Nujol = 2060 cm^{-1} (s) and 2034 cm^{-1} (sh). The spectrum also shows PF_6^- peaks at 839 cm^{-1} (s) and 560 cm^{-1} (m). UV-Vis spectrum in CH_2Cl_2, [$\lambda_{max}(\varepsilon)$]: 394 nm (23,800), 324 nm (22,600). $^{31}P\ \{^1H\}$ NMR spectrum: δ = 10.95 ppm (from 85% H_3PO_4), [^1J(Rh-P) + ^xJ(Rh-P)] = 83.0 Hz. Anal. calcd. for $C_{57}H_{50}Br_3F_6N_2O_2P_5Rh_2$: C, 45.36; H, 3.34; Br, 15.88; N, 1.86. Found: C, 44.75; H, 3.20; Br, 18.22; N, 1.64.

16. Dibromodicarbonyl-μ-4-methylpyrazolatobis[μ-methylenebis[diphenylphosphine]-P:P']-dirhodium(II) Hexafluorophosphate, $[Rh_2Br_2(CO)_2(C_4H_5N_2)(dpm)_2][PF_6]$

Compound 26 was prepared by the same procedure used to make 24. Using Br_2 (ℓ) (0.010 mL, 0.194 mmol) and 8 (253.7 mg, 0.202 mmol) an orange-yellow solid was obtained.

IR spectrum: ν (CO) in Nujol = 2062 cm^{-1} (s) and 2034 cm^{-1} (sh). The spectrum also shows PF_6^- peaks at 839 cm^{-1} (s) and 560 cm^{-1} (m). UV-Vis spectrum in CH_2Cl_2 [$\lambda_{max}(\varepsilon)$]: 386 nm (23,800), 309 nm (19,000), 270 nm (29,900). $^{31}P\{^1H\}$ NMR spectrum: δ = 8.93 ppm (from 85% H_3PO_4), [^1J(Rh-P) + ^xJ(Rh-P)] = 83.0 Hz.

17. Dicarbonyldichloro-μ-4-chloro-pyrazolatobis[μ-methylenebis[diphenylphosphine]-P:P']-dirhodium(II) Hexafluorophosphate, $[Rh_2(CO)_2Cl_2(C_3H_2ClN_2)(dpm)_2][PF_6]\cdot.25\ CH_2Cl_2$

Compound 27 was prepared by adding excess Cl_2 (g) to a stirred methylene chloride solution of 7 (180.0 mg, 0.1448 mmol) at 0°C in the absence of UV light.

The yellow solution was reduced in volume (10 mL) and 50 mL of diethyl ether was added. The yellow solid was collected by filtration, recrystallized from CH_2Cl_2/diethyl ether, then dried in vacuo.

IR spectrum: ν (CO) in Nujol: 2068 cm^{-1} (s) and 2039 cm^{-1} (sh). The spectrum also shows PF_6^- peaks at 839 cm^{-1} (s) and 560 cm^{-1} (m). UV-Vis spectrum in CH_2Cl_2, [$\lambda_{max}(\varepsilon)$]: 357 nm (34,800),

268 nm (38,800). $^{31}P\ \{^{1}H\}$ NMR spectrum: δ = 10.68 ppm (from 85% H_3PO_4), $[^{1}J(Rh\text{-}P) + {}^{x}J(Rh\text{-}P)]$ = 83.0 Hz. Anal. calcd. for $C_{55.25}H_{46.5}Cl_{3.5}F_6N_2O_2P_5Rh_2$: C, 48.43; H, 3.42; Cl, 9.06. Found: C, 40.36; H, 3.07; Cl, 9.08.

18. Dicarbonyldichloro-μ-4-chloro-3,5-dimethylpyrazolatobis[μ-methylenebis[diphenylphosphine]-P:P']-dirhodium(II) Hexafluorophosphate, $[Rh_2(CO)_2Cl_2(C_5H_6ClN_2)(dpm)_2][PF_6]\cdot.25\ CH_2Cl_2$

Compound 28 was prepared by the same procedure used to make 27. Using excess Cl_2 (g) and 6 (183.0 mg, 0.144 mmol) a yellow solid was obtained.

IR spectrum: ν (CO) in Nujol = 2065 cm^{-1} (vs) and 2051 cm^{-1} (s). The spectrum also shows PF_6^- peaks at 839 cm^{-1} (s) and 560 cm^{-1} (m). UV-Vis spectrum in CH_2Cl_2 $[\lambda_{max}(\varepsilon)]$: 363 nm (25,800), 323 nm (25,800), 276 nm (35,000). $^{31}P\ \{^{1}H\}$ NMR spectrum: δ = 13.44 ppm (from 85% H_3PO_4), $[^{1}J(Rh\text{-}P) + {}^{x}J(Rh\text{-}P)]$ = 83.0 Hz. Anal. calcd. for $C_{57.25}H_{49.5}Cl_{3.5}F_6N_2O_2P_5Rh_2$: C, 49.18; H, 3.64; Cl, 8.87. Found: C, 47.82; H, 3.76; Cl, 8.46.

19. Dicarbonyldichloro-μ-4-methylpyrazolatobis[μ-methylenebis[diphenylphosphine]-P:P']-dirhodium(II) Hexafluorophosphate, $[Rh_2(CO)_2Cl_2(C_4H_5N_2)(dpm)_2][PF_6]\cdot.25\ CH_2Cl_2$

Compound 29 was prepared by the same procedure used to make 27. Using excess Cl_2 (g) and 8 (183.5 mg, 0.146 mmol) a yellow solid was obtained.

IR spectrum: ν (CO) in Nujol = 2063 cm^{-1} (s) and 2040 cm^{-1} (sh). The spectrum also shows PF_6^- peaks at 839 cm^{-1} (s) and 560 cm^{-1} (m). UV-Vis spectrum in CH_2Cl_2 [$\lambda_{max}(\varepsilon)$]: 357 nm (21,800), 267 nm (25,900). ^{31}P $\{^1H\}$ NMR spectrum: δ = 11.35 ppm (from 85% H_3PO_4), $[^1J(Rh\text{-}P) + {}^xJ(Rh\text{-}P)]$ = 83.0 Hz. Anal. calcd. for $C_{56.25}H_{48.5}Cl_{2.5}F_6N_2O_2P_5Rh_2$: C, 49.87; H, 3.62; Cl, 6.57. Found: C, 49.19; H, 3.85; Cl, 6.80.

20. Dicarbonyl-μ-4-bromo-3,5-dimethylpyrazolatobis[μ-methylenebis[diphenylphosphine]-P:P']-dirhodium(I) Hexafluorophosphate, $[Rh_2(CO)_2(C_5H_6BrN_2)(dpm)_2][PF_6]$

a. Method 1. A CH_2Cl_2 solution of 25 (109 mg, 0.0722 mmol) with 0.1 M TBAH present was reduced at -0.65 volts (vs SCE) via controlled potential electrolysis. The resulting electrolysis solution was reduced in volume (10 mL) and 50 mL of THF was added which yielded an orange solid. The product was filtered, washed with ether, recrystallized from CH_2Cl_2/THF, and dried in vacuo.

a. Method 2. Compound 10 was produced by the same procedure used to make 6. Using 4-bromo-3,5-dimethylpyrazole (95.8 mg, 0.547 mmol), n-BuLi (0.219 mL, 0.547 mmol), and $[Rh_2(CO)_2(\mu\text{-}Cl)(dpm)_2[PF_6]$)630.9 mg, 0.521 mmol) an orange solid was obtained.

IR spectrum: ν (CO) in Nujol = 1981 cm^{-1} (sh) and 1968 cm^{-1} (s). The spectrum also shows PF_6^- peaks at 839 cm^{-1} (s) and 560

cm^{-1} (m). UV-Vis spectrum in CH_2Cl_2, [$\lambda_{max}(\varepsilon)$]: 487 nm (10,800), 293 nm (11,200). $^{31}P\{^1H\}$ NMR spectrum: δ = 22.1 (from 85% H_3PO_4), [^1J(Rh-P) + ^xJ(Rh-P)] = 129.39 Hz. Anal. calcd. for $C_{57}H_{50}BrF_6N_2O_2P_5Rh_2$: C, 50.73; H, 3.73; Br, 5.92. Found: C, 50.06; H, 4.17; Br, 6.01.

21. Dicarbonyl-μ-4-chloro-3,5-dimethylpyrazolatobis[μ-methylenebis[diphenylphosphine]-P:P']-dirhodium(I) Hexafluorophosphate, $[Rh_2(CO)_2(C_5H_6ClN_2)(dpm)_2][PF_6]\cdot.25\ CH_2Cl_2$

A CH_2Cl_2 solution of 28 (155 mg, 0.111 mmol) with 0.1 M TBAH present was reduced at -0.65 volts (vs SCE) via controlled potential electrolysis. The electrolysis solution was reduced in volume (10 mL) and 30 mL of methanol was added resulting in the precipitation of an orange solid. The solid was filtered, recrystallized from CH_2Cl_2/CH_3OH, and dried in vacuo.

IR spectrum: ν (CO) in Nujol = 1983 cm^{-1} (s) and 1970 cm^{-1} (s). The spectrum also shows PF_6^- peaks at 839 cm^{-1} (s) and 560 cm^{-1} (m). UV-Vis spectrum in CH_2Cl_2, [$\lambda_{max}(\varepsilon)$]: 485 nm (11,500), 296 nm (12,200). $^{31}P\{^1H\}$ NMR spectrum: δ = 22.2 ppm (from 85% H_3PO_4), [^1J(Rh-P) + ^xJ(Rh-P)] = 126.95 Hz. Anal. calcd. for $C_{57.25}H_{50.5}Cl_{1.5}F_6N_2O_2P_5Rh_2$: C, 51.80; H, 3.83; Cl, 4.01. Found: C, 51.41; H, 3.47; Cl, 3.90.

CHAPTER III

RESULTS AND DISCUSSION

Table I lists by number all compounds appearing in the Results and Discussion. An explanation of abbreviations used appears at the end of Table I.

Dinuclear rhodium(I) A-frame complexes (6-11) with the triazolate ion or a pyrazolate derivative situated in the bridgehead position were synthesized by adding the appropriate lithium salt to a THF solution of $[Rh_2(CO)_2(\mu\text{-}Cl)(dpm)_2]PF_6$. Complexes of this type (12-15) can also be synthesized by adding the potassium salt of the appropriate ligand to an acetone suspension of trans-$[Rh_2Cl_2(CO)_2(dpm)_2]$.[33] This latter procedure has been used to prepare complexes (12-15) that have perchlorate as the counter ion.

The $^{31}P\ \{^1H\}$ NMR spectra of complexes 6-15 show a symmetric multiplet featuring the familiar AA'A"A'"XX' pattern, indicating that all four phosphorus atoms are chemically but not magnetically equivalent (Figure 1). The values of $\delta(P)$ (from 85% H_3PO_4) range from 19.2-24.4 ppm for the complexes 6-11 (Table II). The second-order nature of the spectra of these complexes precludes the possibility of obtaining exact coupling constants without computer simulation. The frequency difference between the two major peaks in the NMR spectra is represented by $[^1J(RhP) + {}^xJ(RhP)]$. These values ranged from 127.0-129.4 Hz for the complexes 6-11. The values for

TABLE I

COMPOUND IDENTIFICATION

Compound Number	Compound
1	$[Rh_2(CO)_2(\mu\text{-}CO)(\mu\text{-}Cl)(dpm)_2]PF_6$
2	$[Rh_2(CO)_2(\mu\text{-}Cl)(dpm)_2]PF_6$
3	trans-$Rh_2(CO)_2Cl_2(dpm)_2$
4	$[Rh_2Cl_2(\mu\text{-}CO)(\mu\text{-}Cl)(dpm)_2]PF_6$
5	$Rh_2Cl_3(CO)(\mu\text{-}Cl)(dpm)_2$
6	$[Rh_2(CO)_2(\mu\text{-}3,5\text{-DMP})(dpm)_2]PF_6$
7	$[Rh_2(CO)_2(\mu\text{-pz})(dpm)_2]PF_6$
8	$[Rh_2(CO)_2(\mu\text{-4MP})(dpm)_2]PF_6$
9	$[Rh_2(CO)_2(\mu\text{-Triaz})(dpm)_2PF_6$
10	$[Rh_2(CO)_2(\mu\text{-4B-3,5-DMP})(dpm)_2]PF_6$
11	$[Rh_2(CO)_2(\mu\text{-4Cl-3,5-DMP})(dpm)_2]PF_6 \cdot .25CH_2Cl_2$
12	$[Rh_2(CO)_2(\mu\text{-pz})(dpm)_2]ClO_4$
13	$[Rh_2(CO)_2(\mu\text{-3MP})(dpm)_2]ClO_4$
14	$[Rh_2(CO)_2(\mu\text{-3,5-DMP})(dpm)_2]ClO_4$
15	$[Rh_2(CO)_2(\mu\text{-4B-pz})(dpm)_2]ClO_4$
16	$[Rh_2(CO)_2I_2(\mu\text{-3,5-DMP})(dpm)_2]PF_6$
17	$[Rh_2(CO)_2I_2(\mu\text{-pz})(dpm)_2]PF_6$
18	$[Rh_2(CO)_2I_2(\mu\text{-4MP})(dpm)_2]PF_6$
19	$[Rh_2(CO)_2I_2(\mu\text{-Triaz})(dpm)_2]PF_6$
20	$[Rh_2(CO)_2I_2(\mu\text{-pz})(dpm)_2]ClO_4$

TABLE I (Continued)

Compound Number	Compound
21	$[Rh_2(CO)_2I_2(\mu\text{-}3MP)(dpm)_2]ClO_4$
22	$[Rh_2(CO)_2I_2(\mu\text{-}3,5\text{-}DMP)(dpm)_2]ClO_4$
23	$[Rh_2(CO)_2I_2(\mu\text{-}4B\text{-}pz)(dpm)_2]ClO_4$
24	$[Rh_2Br_2(CO)_2(\mu\text{-}4B\text{-}pz)(dpm)_2]PF_6$
25	$[Rh_2Br_2(CO)_2(\mu\text{-}4B\text{-}3,5\text{-}DMP)(dpm)_2]PF_6$
26	$[Rh_2Br_2(CO)_2(\mu\text{-}4MP)(dpm)_2]PF_6$
27	$[Rh_2(CO)_2Cl_2(\mu\text{-}4Cl\text{-}pz)(dpm)_2]PF_6\cdot.25CH_2Cl_2$
28	$[Rh_2(CO)_2Cl_2(\mu\text{-}4Cl\text{-}3,5\text{-}DMP)(dpm)_2]PF_6\cdot.25CH_2Cl_2$
29	$[Rh_2(CO)_2Cl_2(\mu\text{-}4MP)(dpm)_2]PF_6\cdot.25CH_2Cl_2$

Abbreviations:

dpm = $\mu\text{-}(C_6H_5)_2PCH_2P(C_6H_5)_2$

3,5-DMP = $C_5H_7N_2^-$

pz = $C_3H_3N_2^-$

4MP = $C_4H_5N_2^-$

Triaz = $C_2H_2N_3^-$

4-B-3,5-DMP = $C_5H_6BrN_2^-$

4-Cl-3,5-DMP = $C_5H_6ClN_2^-$

4-B-pz = $C_3H_2BrN_2^-$

3MP = $C_4H_5N_2^-$

4-Cl-pz = $C_3H_2ClN_2^-$

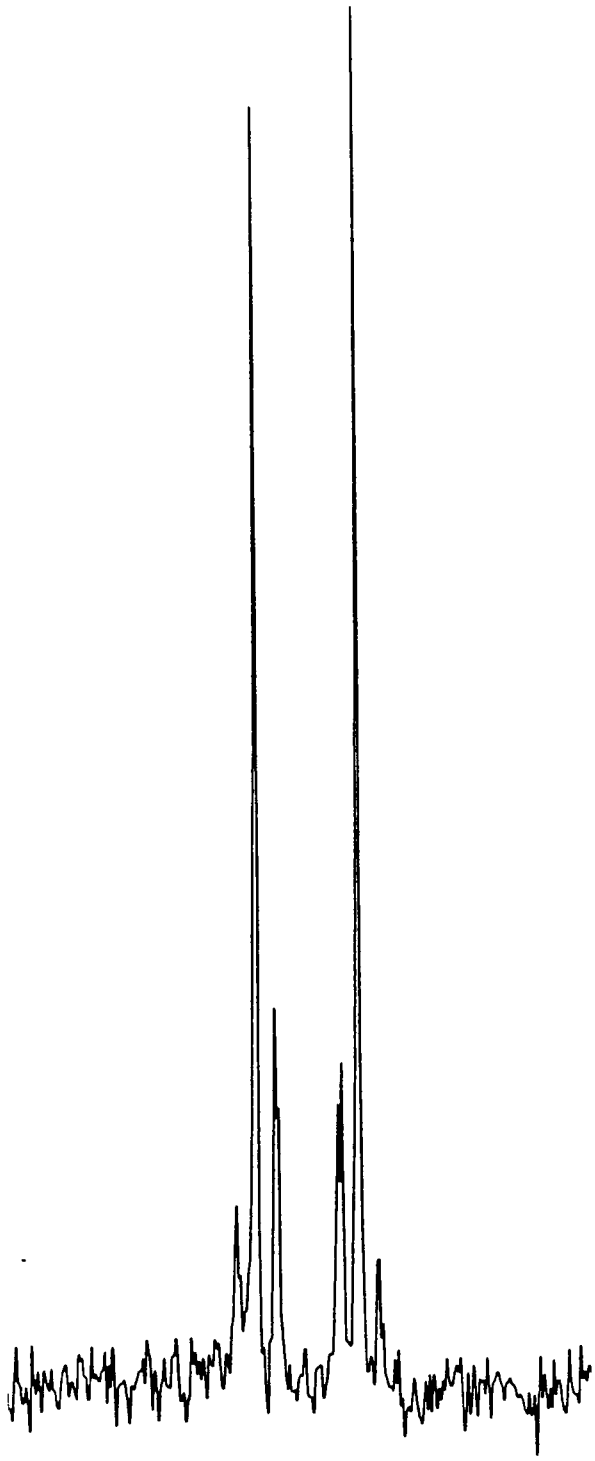


Figure 1. The $^{31}P\{^{1}H\}$ NMR spectrum of $[Rh_2(CO)_2(\mu\text{-}3,5\text{-DMP})(dpm)_2]PF_6$, 6.

TABLE II

$^{31}P\{^{1}H\}$ NMR SPECTRAL DATA FOR SELECTED COMPOUNDS 6-11

Number	Compound	$\delta(p)^a$, ppm	$[^1J(Rh-P)+^xJ(Rh-P)]^b$, Hz
6	$[Rh_2(CO)_2(\mu\text{-}3,5\text{-DMP})(dpm)_2]PF_6$	22.7	129.0
7	$[Rh_2(CO)_2(\mu\text{-pz})(dpm)_2]PF_6$	19.2	129.0
8	$[Rh_2(CO)_2(\mu\text{-4MP})(dpm)_2]PF_6$	24.4	129.0
9	$[Rh_2(CO)_2(\mu\text{-Triaz})(dpm)_2]PF_6$	23.5	127.0
10	$[Rh_2(CO)_2(\mu\text{-4B-}3,5\text{-DMP})(dpm)_2]PF_6$	22.1	129.0
11	$[Rh_2(CO)_2(\mu\text{-4Cl-}3,5\text{-DMP})(dpm)_2]PF_6 \cdot .25CH_2Cl_2$	22.2	127.0

[a]Chemical shifts were measured with respect to 85% H_3PO_4 as the external reference.

[b]Coupling constants ± 0.6 Hz.

$\delta(P)$ and $[^1J(RhP) + {}^xJ(RhP)]$ are in the usual ranges for related Rh-dpm complexes.[1,7,9,12,14,15,18,19,22]

The electronic spectra of the rhodium(I) hexafluorophosphate and perchlorate complexes (6-15) have λ_{max} values in the range 484-495 nm, with molar absorption coefficients in the range of 9,000-20,000 ℓ mol^{-1} cm^{-1} (Table III).[33] These metal-centered low energy absorption bands can be described as proximity shifted bands resulting from the electronic transition, $1b_{1u}(4d_{z2}) \rightarrow 2a_g(5p_z)$ (see Figure 2).

Oxidation of the hexafluorophosphate and perchlorate complexes, 6-15, by molecular iodine (1:1 mol ratio) resulted in the formation of red-brown solids (16-23) having the general structure shown in Figure 3. The electronic spectra of complexes 16-19 (Table IV) are consistent with the data reported for complexes 20-23[33] in that they display two to three intense absorptions in the 400-515 nm range.

These iodo complexes exhibit terminal carbonyl stretching frequencies approximately 100 cm^{-1} higher than those of the starting materials (Table V). The observed shift of the carbonyl stretching frequencies in converting from rhodium(I) to rhodium(II) is due to a decrease of electron density on the rhodium, thereby diminishing the amount of metal $d\pi$ electron density CO must accept into its π^* orbitals. This decrease in antibonding electron density increases the CO bond order and hence the CO stretching frequency. The shifts in the values of $\nu(CO)$ are consistent with related systems.[11,24]

The $^{31}P\{^1H\}$ NMR spectral patterns for the complexes 16-23 are similar to those observed for the related starting materials.

TABLE III

UV-VIS SPECTRAL DATA FOR SELECTED COMPOUNDS 6-11

Number	Compound	λ_{max}, nm (ε)
6	$[Rh_2(CO)_2(\mu\text{-}3,5\text{-}DMP)(dpm)_2]PF_6$	484 (20,500)
7	$[Rh_2(CO)_2(\mu\text{-}pz)(dpm)_2]PF_6$	492 (15,200)
8	$[Rh_2(CO)_2(\mu\text{-}4MP)(dpm)_2]PF_6$	493 (20,300)
9	$[Rh_2(CO)_2(\mu\text{-}Triaz)(dpm)_2]PF_6$	487 (19,000)
10	$[Rh_2(CO)_2(\mu\text{-}4B\text{-}3,5\text{-}DMP)(dpm)_2]PF_6$	487 (10,800), 293 (11,200)
11	$[Rh_2(CO)_2(\mu\text{-}4Cl\text{-}3,5\text{-}DMP)(dpm)_2]PF_6 \cdot .25\ CH_2Cl_2$	485 (11,500), 296 (12,200)

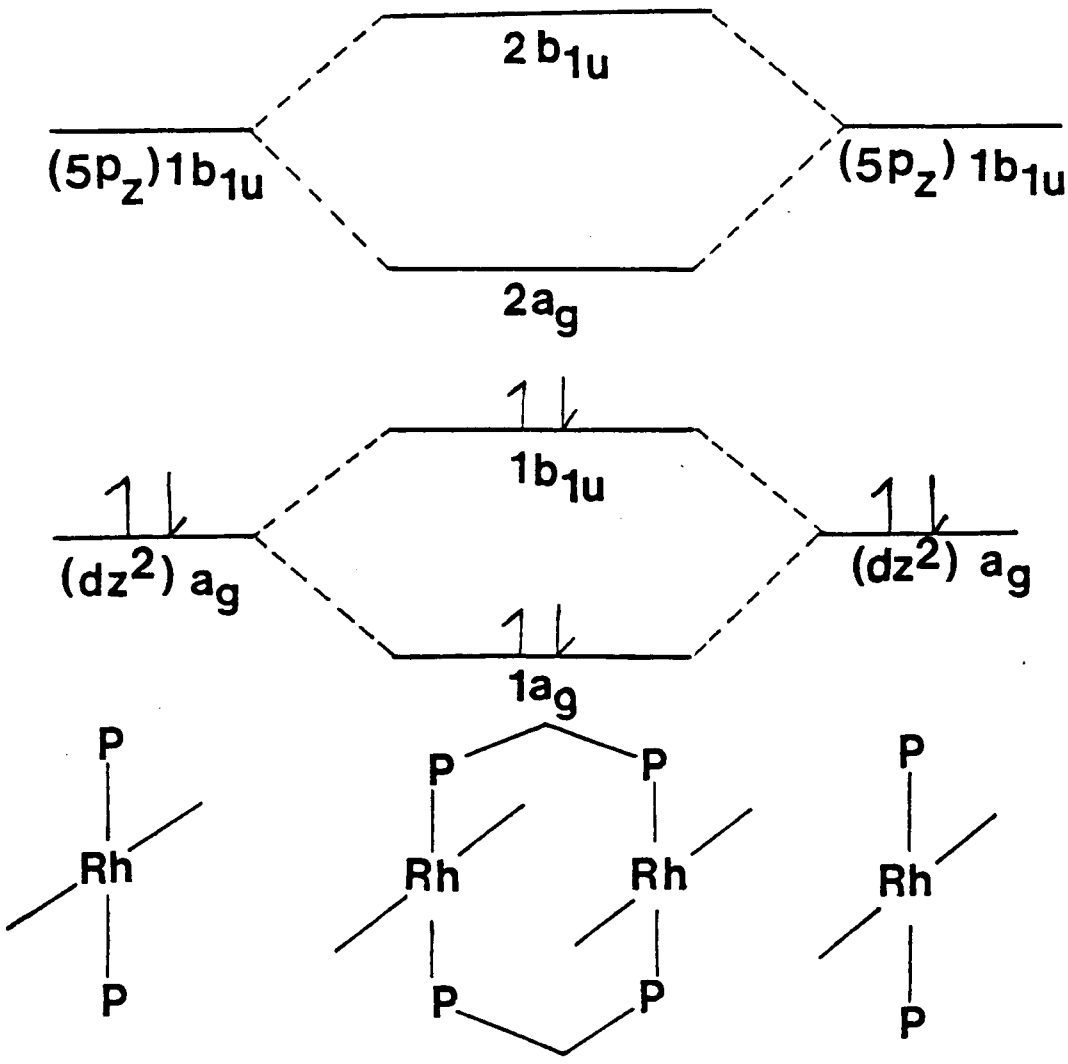
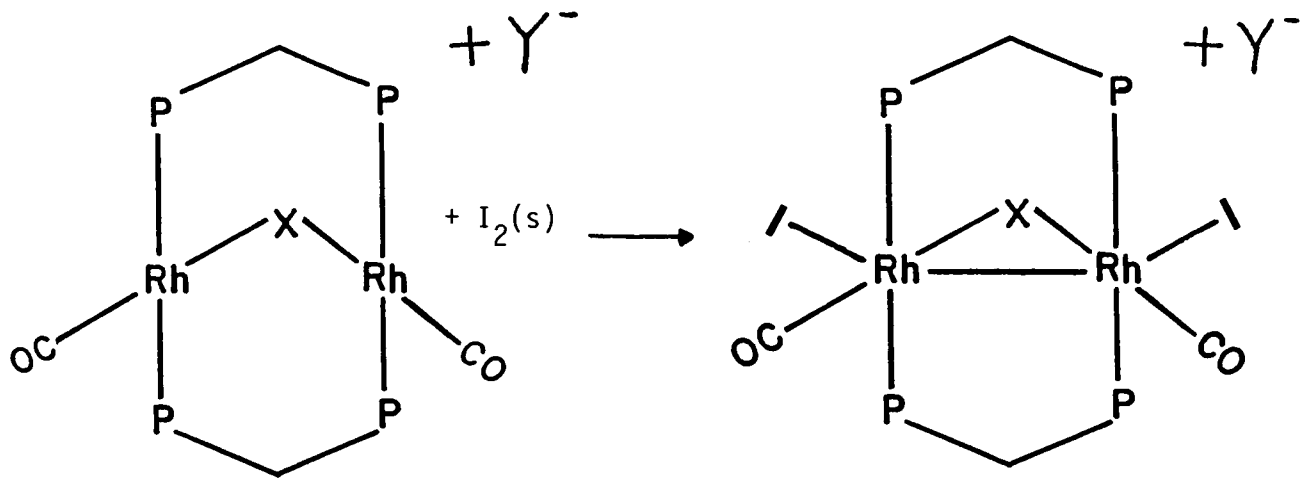


Figure 2. Simplified molecular orbital diagram showing the orbital interactions resulting from face-to-face approach of two square-planar Rh(I) units.



X^- = $Triaz^-$, pz^-, $3,5\text{-}DMP^-$, $4MP^-$, $3MP^-$, $4B\text{-}pz^-$

Y^- = PF_6^-, ClO_4^-

Figure 3. Oxidation of the hexafluorophosphate and perchlorate complexes, 6-15, by molecular iodine (1:1 mol ratio) to form the complexes, 16-23.

TABLE IV

UV-VIS SPECTRAL DATA IN THE 500-515 nm RANGE FOR SELECTED COMPOUNDS

No.	Compound	λ_{max}, nm (ε)
16	$[Rh_2(CO)_2I_2(\mu\text{-}3,5\text{-}DMP)(dpm)_2]PF_6$	511 (15,000), 450 (19,400), 399 (21,600)
17	$[Rh_2(CO)_2I_2(\mu\text{-}pz)(dpm)_2]PF_6$	509 (13,600), 440 (18,700), 410 (19,400)
18	$[Rh_2(CO)_2I_2(\mu\text{-}4MP)(dpm)_2PF_6$	508 (18,300), 436 (25,400), 411 (25,600)
19	$[Rh_2(CO)_2I_2(\mu\text{-}Triaz)(dpm)_2PF_6$	511 (15,000), 443 (21,400), 406 (24,500)

TABLE V

IR SPECTRAL DATA FOR SELECTED COMPOUNDS

No.	Compound	ν(CO)[a], cm^{-1}
6	$[Rh_2(CO)_2(\mu\text{-}3,5\text{-DMP})(dpm)_2]PF_6$	1975 (s), 1962 (s)
7	$[Rh_2(CO)_2(\mu\text{-pz})(dpm)_2]PF_6$	1988 (s), 1967 (s)
8	$[Rh_2(CO)_2(\mu\text{-4MP})(dpm)_2]PF_6$	1984 (s), 1973 (s)
9	$[Rh_2(CO)_2(\mu\text{-Triaz})(dpm)_2]PF_6$	1991 (s)
10	$[Rh_2(CO)_2(\mu\text{-4B-3,5-DMP})(dpm)_2]PF_6$	1981 (sh), 1968 (s)
11	$[Rh_2(CO)_2(\mu\text{-4Cl-3,5-DMP})(dpm)_2]PF_6 \cdot .25CH_2Cl_2$	1983 (s), 1970 (s)
12	$[Rh_2(CO)_2(\mu\text{-pz})(dpm)_2]ClO_4$	2000 (vs), 1986 (sh)[b]
13	$[Rh_2(CO)_2(\mu\text{-3MP})(dpm)_2]ClO_4$	1998 (vs), 1983 (sh)[b]
14	$[Rh_2(CO)_2(\mu\text{-3,5-DMP})(dpm)_2]ClO_4$	1995 (vs), 1980 (sh)[b]
15	$[Rh_2(CO)_2(\mu\text{-4B-pz})(dpm)_2]ClO_4$	2002 (vs), 1988 (sh)[b]
16	$[Rh_2(CO)_2I_2(\mu\text{-3,5-DMP})(dpm)_2]PF_6$	2056 (s)
17	$[Rh_2(CO)_2I_2(\mu\text{-pz})(dpm)_2]PF_6$	2065 (s), 2031 (m)

TABLE V (Continued)

No.	Compound	$\nu(CO)^a$, cm^{-1}
18	$[Rh_2(CO)_2I_2(\mu\text{-}4MP)(dpm)_2]PF_6$	2063 (s), 2031 (sh)
19	$[Rh_2(CO)_2I_2(\mu\text{-}Triaz)(dpm)_2]PF_6$	2063 (s), 2031 (s)
20	$[Rh_2(CO)_2I_2(\mu\text{-}pz)(dpm)_2]ClO_4$	2052 (s)[b]
21	$[Rh_2(CO)_2I_2(\mu\text{-}3MP)(dpm)_2]ClO_4$	2056 (s)[b]
22	$[Rh_2(CO)_2I_2(\mu\text{-}3,5\text{-}DMP)(dpm)_2]ClO_4$	2055 (s)[b]
23	$[Rh_2(CO)_2I_2(\mu\text{-}4B\text{-}pz)(dpm)_2]ClO_4$	2056 (s)[b]

[a]Nujol mull unless otherwise stated.

[b]Dichloromethane; taken from reference 33.

On the other hand, the values for $\delta(P)$ and $[^{1}J(RhP) + {}^{X}J(RhP)]$ decrease significantly from averages of 22.4 ppm and 128.5 Hz for the Rh(I) starting materials, to averages of 5.4 ppm and 83.6 Hz for the Rh(II) iodo systems, 16-19, respectively (Tables II and VI).

The crystal structure of $[Rh_2(CO)_2(\mu\text{-}3,5\text{-}DMP)(dpm)_2]ClO_4$[33] involves a square planar arrangement of ligands around each Rh atom consisting of two trans P donors (from the dpm ligands), a carbon atom (from the CO), and a nitrogen atom (from the 3,5-DMP ligand). No evidence exists for a metal-metal bond in this 16-electron system since this species has a Rh---Rh separation of 3.060 Å. However, there does appear to be a weak metal-metal interaction since the two rhodium atoms are distorted toward each other out of the two rhodium-containing square planes by 0.0583 and 0.0553 Å.

The crystal structure of $[Rh_2I_2(CO)_2(\mu\text{-}3,5\text{-}DMP)(dpm)_2]ClO_4$[33] shows an octahedral arrangement of ligands around each rhodium atom consisting of two trans P donors, a carbon atom from the CO, a nitrogen atom, an iodine atom, and the other rhodium atom. This 18-electron system possesses one of the shortest Rh-Rh bond lengths ever reported (2.725 Å). Rh-Rh distances for similar A-frame complexes range from 2.745-2.842 Å.[22]

Some of the differences between the structural parameters in $[Rh_2(CO)_2(\mu\text{-}3,5\text{-}DMP)(dpm)_2]ClO_4$ and $[Rh_2I_2(CO)_2(\mu\text{-}3,5\text{-}DMP)(dpm)_2]ClO_4$ include the dramatic shortening of the metal-metal separation in converting from Rh(I) to Rh(II). There also appears to be a lengthening of the distance from rhodium to ligand donor atom in the Rh(II) complex in comparison to the Rh(I) complex (Rh-P, 2.319 and 2.393 Å (avg.); Rh-C, 1.760 and 1.802 Å (avg.); and Rh-N, 2.075 and 2.091 Å

TABLE VI

$^{31}P\{^{1}H\}$ NMR SPECTRAL DATA FOR SELECTED COMPOUNDS 16-19

No.	Compound	$\delta(P)^a$ ppm	$[^1J(Rh-P) + {}^xJ(Rh-P)]^b$ Hz
16	$[Rh_2(CO)_2I_2(\mu\text{-}3,5\text{-}DMP)(dpm)_2]PF_6$	6.4	85.0
17	$[Rh_2(CO)_2I_2(\mu\text{-}pz)(dpm)_2]PF_6$	4.8	83.0
18	$[Rh_2(CO)_2I_2(\mu\text{-}4MP)(dpm)_2]PF_6$	4.9	83.0
19	$[Rh_2(CO)_2I_2(\mu\text{-}Triaz)(dpm)_2]PF_6$	5.3	83.0

[a]Chemical shifts were measured with respect to 85% H_3PO_4 as the external reference.

[b]Coupling constants ± 0.6 Hz.

(avg.), for the Rh(I) and Rh(II) complexes, respectively). It appears that longer Rh-P bond distances are present in complexes whose metals are in higher formal oxidation states.[33]

Oxidation of the hexafluorophosphate complexes 6-9 by molecular bromine (1:1 mol ratio) or excess chlorine results in the formation of orange or yellow solids (24-29) exhibiting terminal carbonyl stretching frequencies similar to those observed for the analogous iodo complexes, 16-19.

These Rh(II) bromo and chloro complexes, 24-29, display a symmetrical $^{31}P\{^{1}H\}$ NMR pattern indicative of the familiar AA'A"A'"XX' spin system. (NOTE: It was not possible to obtain a $^{31}P\{^{1}H\}$ NMR spectrum of either the bromo or chloro triazolate-bridged complexes due to the inability to obtain an analytically pure sample.) The values of $[^{1}J(RhP) + {}^{X}J(RhP)]$ for the bromo and chloro derivatives are almost identical to those for the related iodo complexes, 16-18. However, the chemical shifts for bromo and chloro complexes are shifted downfield in comparison to the analogous iodo complexes, 16-18 (Tables VI and VII).

The average $\delta(P)$ values for the bromo complexes (24-26) and chloro complexes (27-29) were 4.2 ppm and 6.4 ppm, respectively, farther downfield from their iodo analogues (16-18). On the basis of polarizability, one would expect to observe the opposite trend in chemical shifts for the iodo, bromo, and chloro complexes. Since the iodide ligand is more polarizable than the bromide ligand and the chloride ligand, one would expect there to be greater electron

TABLE VII

$^{31}P\{^{1}H\}$ NMR SPECTRAL DATA FOR SELECTED COMPOUNDS 24-29

No.	Compound	$\delta(P)^a$ ppm	$[^1J(Rh-P) + {}^xJ(Rh-P)]^b$ Hz
24	$[Rh_2Br_2(CO)_2(\mu\text{-}4B\text{-}pz)(dpm)_2]PF_6$	8.9	81.0
25	$[Rh_2Br_2(CO)_2(\mu\text{-}4B\text{-}3,5\text{-}DMP)(dpm)_2]PF_6$	11.0	83.0
26	$[Rh_2Br_2(CO)_2(\mu\text{-}4MP)(dpm)_2]PF_6$	8.9	83.0
27	$[Rh_2(CO)_2Cl_2(\mu\text{-}4Cl\text{-}pz)(dpm)_2]PF_6\cdot.25CH_2Cl_2$	10.7	83.0
28	$[Rh_2(CO)_2Cl_2(\mu\text{-}4Cl\text{-}3,5\text{-}DMP)(dpm)_2]PF_6\cdot.25CH_2Cl_2$	13.4	83.0
29	$[Rh_2(CO)_2Cl_2(\mu\text{-}4MP)(dpm)_2]PF_6\cdot.25CH_2Cl_2$	11.4	83.0

[a]Chemical shifts were measured with respect to 85% H_3PO_4 as the external reference.

[b]Coupling constants ± 0.6 Hz.

density around the rhodium in complexes containing more polarizable ligands. Therefore, one would expect the chemical shifts for the Rh(II) iodo complexes to approach those observed for the Rh(I) starting materials. However, it appears that other factors play a more important role in affecting the phosphorous electronic environment in these halogenated Rh(II) systems. The smaller and more electronegative halides appear to deshield the phosphorus atoms on the dpm ligands resulting in a downfield chemical shift.

The electronic spectra of the bromo and chloro Rh(II) complexes, 24-29, show two or three intense absorptions in the 270-390 nm range for the bromo species, and two or three intense absorptions in the 270-360 nm range for the chloro species (Table VIII).

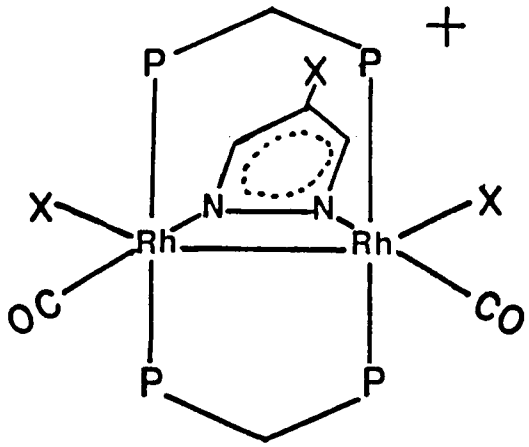
During our investigations on the bromination and chlorination of the 3,5-DMP and pz complexes, 6 and 7, it became apparent that the 3,5-DMP and pz ligands were brominated or chlorinated at the four position on the ring. Proposed structures for the products obtained from the bromination and chlorination of complexes 6-8 are shown in Figure 4.

The reduction of the complex $[Rh_2Br_2(CO)_2(\mu\text{-}4B\text{-}3,5\text{-}DMP)(dpm)_2]PF_6$, 25, at -0.65 V via controlled potential electrolysis results in an orange complex that exhibits two terminal carbonyl stretching frequencies at 1981 (sh) cm^{-1} and 1968 (s) cm^{-1}. The $^{31}P\{^1H\}$ NMR spectrum exhibits the AA'A"A'"XX' pattern with $\delta(P)$ = 22.1 ppm and $[^1J(RhP) + {}^XJ(RhP)]$ = 129.39 Hz. The electronic spectrum of the reduced hexafluorophosphate complex shows two bands at 487 and 293 nm,

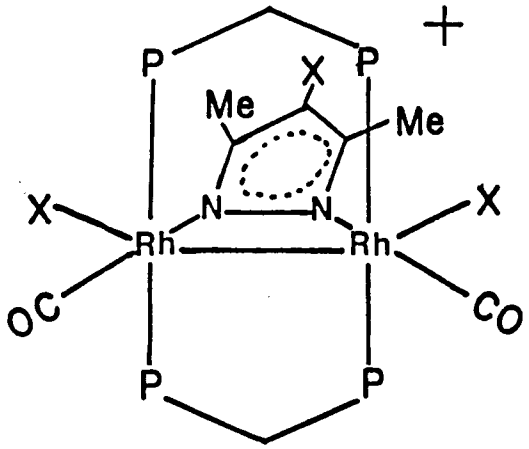
TABLE VIII

UV-VIS SPECTRAL DATA FOR SELECTED COMPOUNDS 24-29

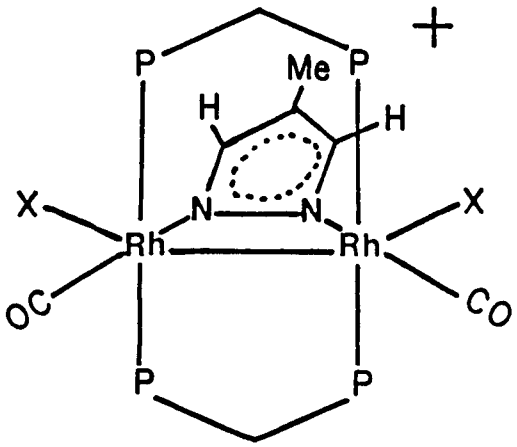
No.	Compound	λ_{max}, nm, (ϵ)
24	$[Rh_2Br_2(CO)_2(\mu\text{-}4B\text{-}pz)(dpm)_2]PF_6$	387 (20,700), 309 (22,500), 267 (28,900)
25	$[Rh_2Br_2(CO)_2(\mu\text{-}4B\text{-}3,5\text{-}DMP(dpm)_2]PF_6$	394 (23,800), 324 (22,600)
26	$[Rh_2Br_2(CO)_2(\mu\text{-}4MP)(dpm)_2]PF_6$	386 (23,800), 309 (19,000), 270 (29,900)
27	$[Rh_2(CO)_2Cl_2(\mu\text{-}4Cl\text{-}pz)(dpm)_2]PF_6\cdot.25CH_2Cl_2$	357 (34,800), 268 (38,800)
28	$[Rh_2(CO)_2Cl_2(\mu\text{-}4Cl\text{-}3,5\text{-}DMP)(dpm)_2]PF_6\cdot.25CH_2Cl_2$	363 (25,800), 323 (25,800), 276 (35,000)
29	$[Rh_2(CO)_2Cl_2(\mu\text{-}4MP)(dpm)_2]PF_6\cdot.25CH_2Cl_2$	357 (21,800), 267 (25,900)



24: X = Br
27: X = Cl



25: X = Br
28: X = Cl



26: X = Br
29: X = Cl

Figure 4. Products obtained from bromination or chlorination of complexes, 6-8.

with molar absorption coefficients of 10,800 and 11,200 $\ell\ mol^{-1}\ cm^{-1}$, respectively. The elemental analysis confirmed the existence of one bromine per molecule of complex. These data are identical to that obtained for the complex $[Rh_2(CO)_2(\mu\text{-}4B\text{-}3,5\text{-}DMP)(dpm)_2]PF_6$, 10, thereby confirming the presence of a bromine atom in the 4-position of the 3,5-DMP ligand in the reduced complex. Based on these data and elemental analysis it appears that the product before reduction can be formulated as 25.

The reduction of the related chloro complex $[Rh_2(CO)_2Cl_2(\mu\text{-}4Cl\text{-}3,5\text{-}DMP)(dpm)_2]PF_6 \cdot .25\ CH_2Cl_2$, 28, at -0.65 V via controlled potential electrolysis results in an orange complex that exhibits two terminal carbonyl stretching frequencies at 1983 (s) cm^{-1} and 1970 (s) cm^{-1} and features a $^{31}P\ \{^1H\}$ NMR spectrum and electronic spectrum almost identical to that observed for the related 4-B-3,5-DMP complex, 10.

Based on the presence of the AA'A"A'"XX' pattern in the $^{31}P\ \{^1H\}$ NMR spectrum and the elemental analysis, this reduction product is formulated as $[Rh_2(CO)_2(\mu\text{-}4Cl\text{-}3,5\text{-}DMP)(dpm)_2]PF_6 \cdot .25\ CH_2Cl_2$, 11. Though there was no spectroscopic evidence for the presence of CH_2Cl_2 of solvation, the elemental analysis is consistent with a .25 mole of CH_2Cl_2 per rhodium dimer. In cases where crystal structures on analogous dinuclear rhodium complexes have been done, the majority have been shown to contain four dimeric units per unit cell. Therefore, if each unit cell contains a molecule of CH_2Cl_2, that represents a .25 mole of CH_2Cl_2 per dimeric unit.

In view of the ability of the complex $[Rh_2(CO)_2(\mu\text{-}3,5\text{-}DMP(dpm)_2]PF_6$, 6, to undergo transannular oxidative addition of bromine and chlorine as well as substitution of bromine or chlorine in the 4-position on the 3,5-DMP ligand, it was believed that the oxidative addition and substitution reaction might also occur with the related pyrazolate complex, 7. Based on the presence of the AA'A"A'"XX' pattern in the $^{31}P\ \{^1H\}$ NMR spectrum and the elemental analysis, this product is formulated as $[Rh_2(CO)_2Cl_2(\mu\text{-}4Cl\text{-}pz)(dpm)_2]PF_6 \cdot .25\ CH_2Cl_2$, 27. The presence of CH_2Cl_2 of solvation can be rationalized as before.

The $^{31}P\ \{^1H\}$ NMR spectrum of the related bromo complex $[Rh_2Br_2(CO)_2(\mu\text{-}4B\text{-}pz)(dpm)_2]PF_6$, 24, showed the presence of impurities, therefore the reaction was done at -30°C and the product was subsequently precipitated at this temperature. Although there were still impurity peaks present in the $^{31}P\ \{^1H\}$ NMR spectrum of this product, they appeared to be less significant (Figure 5). Therefore, it also appears that this complex is brominated in the 4-position on the pz ligand.

Figure 6 illustrates a typical cyclic voltammogram observed for the complexes 6-9 in CH_2Cl_2 and 0.1 M TBAH. Analysis of the voltammetric data (Table IX) indicates the following: (1) the midpoint potentials, $E_{1/2}$ were invariant with sweep rate; (2) the values of ΔE, the potential difference between E_{pa} and E_{pc}, increase as the sweep rate increases; (3) the ratio of the peak currents (i_{pc}/i_{pa}) were essentially unity; and (4) the values for i_{pa} were proportional

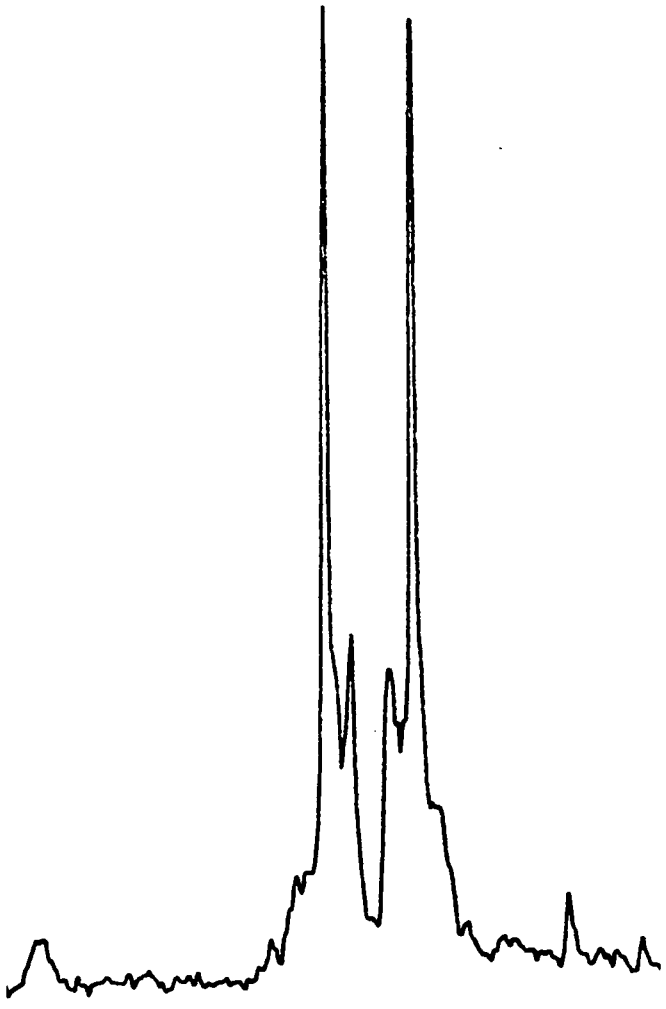
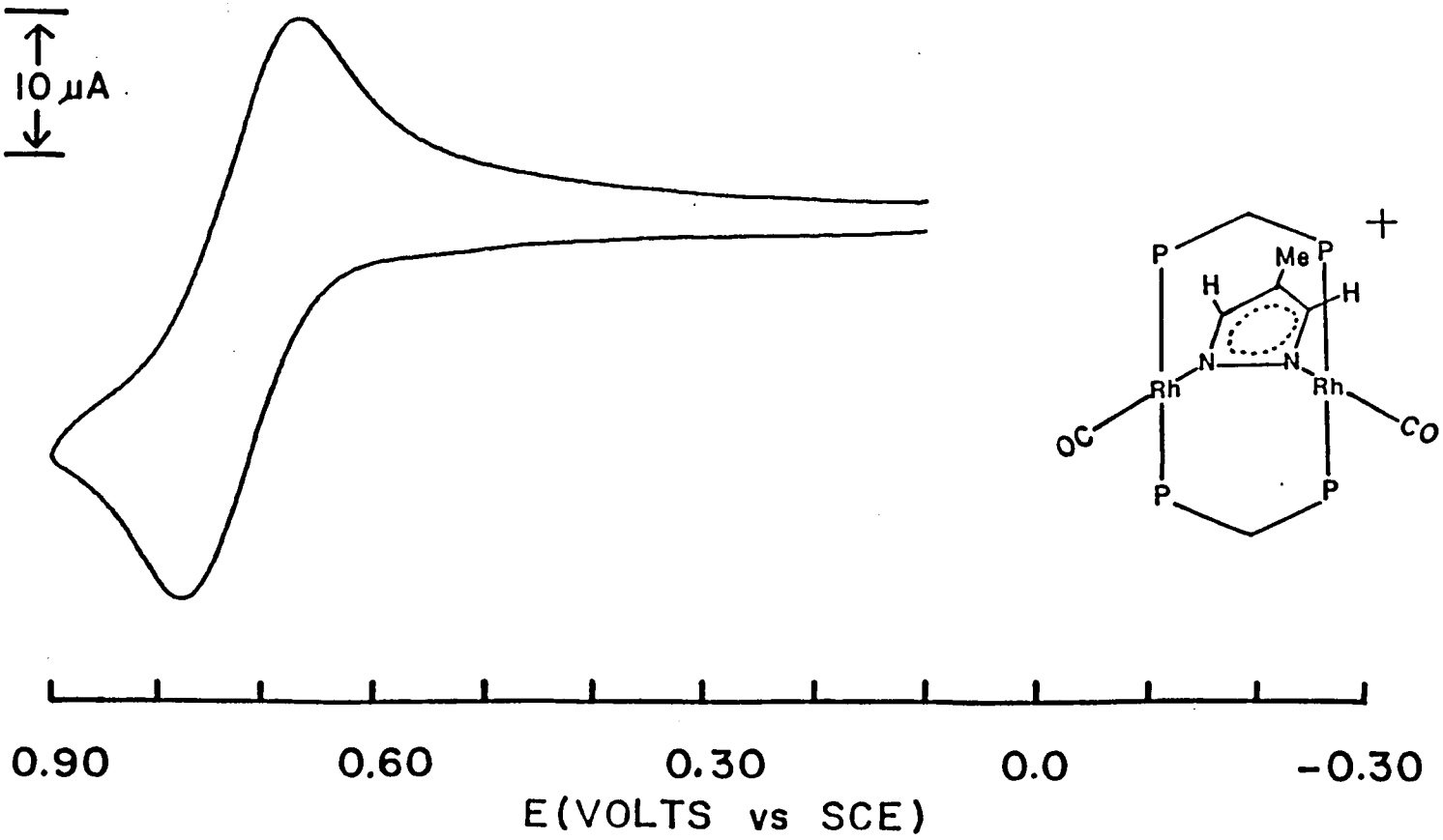


Figure 5. The $^{31}P\{^{1}H\}$ NMR spectrum of $[Rh_2Br_2(CO)_2(\mu\text{-}4B\text{-}pz)(dpm)_2]PF_6$, 24.



Conditions: Conc. 5.0 x 10^{-4}M; 0.10 M TBAH/CH_2Cl_2; sweep rate, 100 mV/sec; SCE.

Figure 6. Cyclic voltammogram of 8.

TABLE IX

CYCLIC VOLTAMMETRIC DATA FOR THE COMPLEXES, 6-9[a]

Complex	V[b]	E_{pa}, V	E_{pc}, V	ΔE, V	$E_{1/2}$, V	i_{pc}/i_{pa}
$[Rh_2(CO)_2(\mu\text{-}3,5\text{-DMP})(dpm)_2]PF_6$, 6	50	0.78	0.68	0.10	0.73	1.0
	100	0.78	0.67	0.11	0.72	
	200	0.81	0.67	0.14	0.74	
	300	0.82	0.67	0.15	0.74	
	400	0.83	0.67	0.16	0.75	
	500	0.84	0.67	0.17	0.76	
$[Rh(CO)_2(\mu\text{-pz})(dpm)_2]PF_6$, 7	50	0.81	0.70	0.11	0.76	1.02
	100	0.82	0.70	0.12	0.76	
	200	0.84	0.68	0.16	0.76	
	500	0.86	0.66	0.20	0.76	
$[Rh_2(CO)_2(\mu\text{-4MP})(dpm)_2]PF_6$, 8	50	0.77	0.68	0.09	0.72	1.0
	100	0.78	0.67	0.11	0.72	
	200	0.79	0.66	0.13	0.72	
	300	0.80	0.66	0.14	0.73	
	400	0.81	0.66	0.15	0.74	
	500	0.82	0.65	0.17	0.74	

TABLE IX (Continued)

Complex	V[b]	E_{pa}, V	E_{pc}, V	ΔE, V	$E_{1/2}$, V	i_{pc}/i_{pa}
$[Rh_2(CO)_2(\mu\text{-Triaz})(dpm)_2]PF_6$, 9	50	0.93	0.83	0.10	0.88	0.98
	100	0.94	0.82	0.12	0.88	
	200	0.96	0.81	0.15	0.88	
	300	0.97	0.80	0.17	0.88	
	400	0.98	0.80	0.18	0.89	
	500	0.98	0.79	0.19	0.88	

[a]All potentials are measured vs SCE.

[b]Sweep rate in millivolts sec^{-1}.

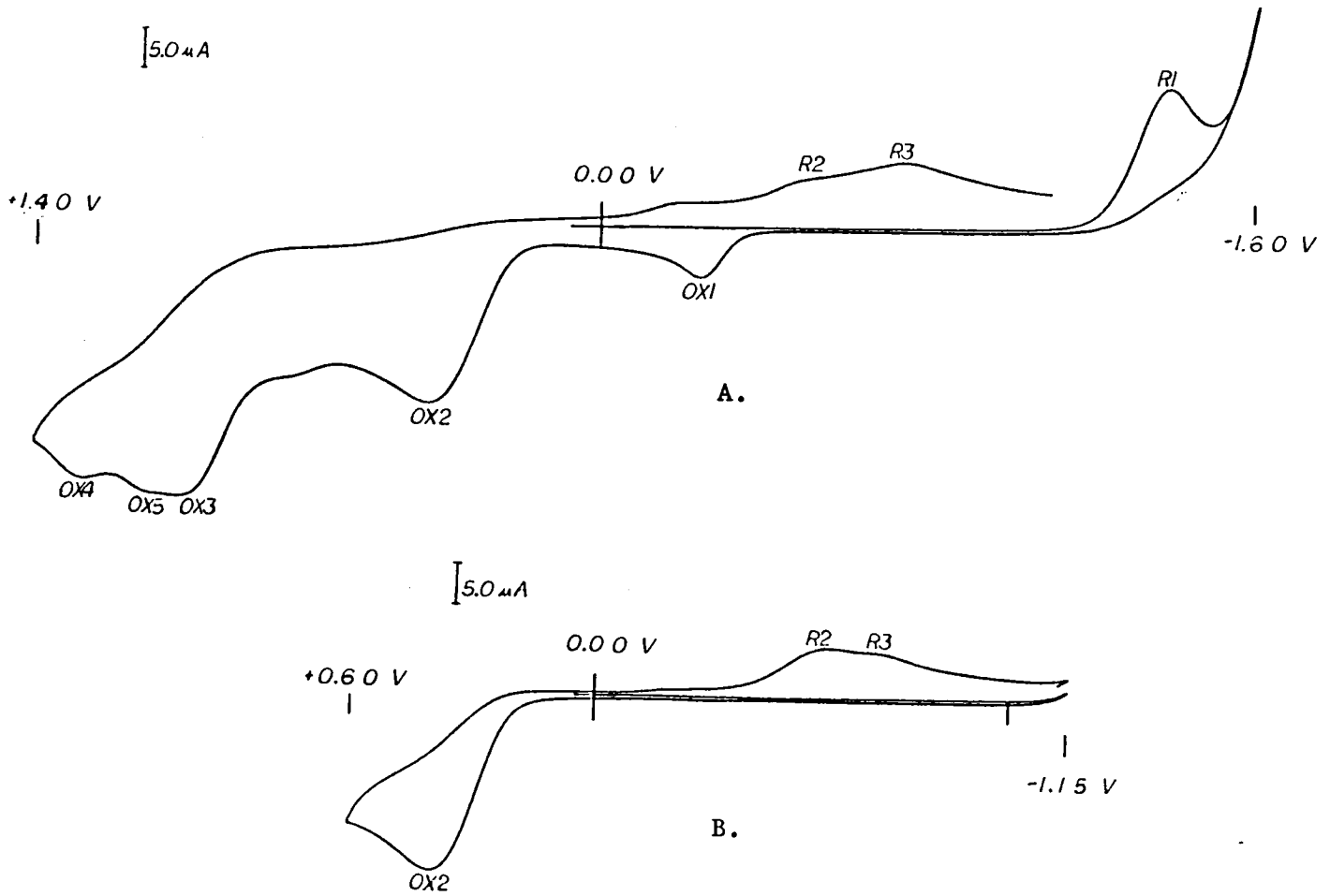
to the square root of the potential sweep rate. This behavior is consistent with a quasi-reversible electron-transfer process.[26,34,35] Further electrochemical investigations are being conducted by another member of the research group.

CHAPTER IV

ELECTROSYNTHESIS OF RHODIUM(II) COMPLEXES

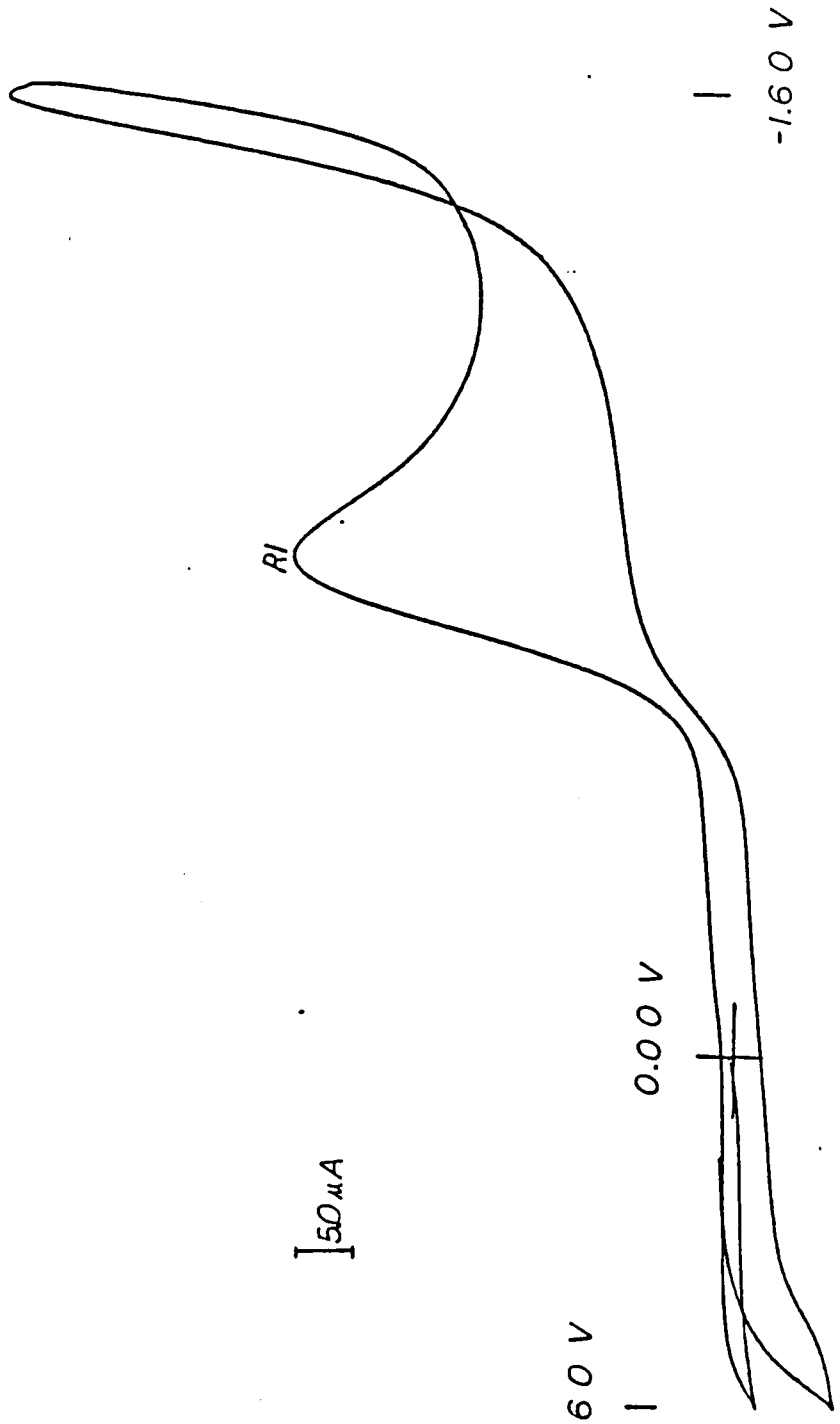
Electrochemical synthesis via controlled potential electrolysis oftentimes allows one to synthesize complexes which might be difficult or impossible to obtain by ordinary chemical processes. The ease with which rhodium(I) dimers undergo oxidative-addition reactions has recently been investigated by Womack.[23] In his study he found that in the presence of a coordinating ligand, the rhodium (I) dimers seem to be more easily oxidized. Figure 7 shows the cyclic voltammogram of 3 (trans-$Rh_2Cl_2(CO)_2(dpm)_2$) in CH_2Cl_2 containing 0.1 M TBAH and a 10-fold molar excess of TBAC. The oxidation wave (Ox5) at +1.10 volts is due to free Cl^-.[32] Upon isolation of the oxidation wave (Ox2) (Figure 7) it becomes clear that the reduction waves at -0.50 volts (R2) and -0.75 volts (R3) are associated with oxidation of the parent species.

Using exhaustive coulometry at +0.70 volts, Ox2 of Figure 7 disappears resulting in the voltammogram shown in Figure 8. The coulometry indicates that oxidation is a two-electron process, giving rise to a product having a reduction wave (R1) at -0.82 volts. When the resulting brown oxidized solution is reduced to a small volume (5 mL) and treated with methanol to remove the TBAH and TBAC, a green product is obtained. The IR spectrum of the isolated green product shows a single peak for ν(CO) at 1799 cm^{-1} (s) which is indicative of a bridging CO. The $^{31}P\{^1H\}$ NMR spectrum



Conditions A and B: Conc. 5.0 x 10^{-4} M; 0.10 M TBAH/CH_2Cl_2; sweep rate 100 mV sec^{-1}; SCE.

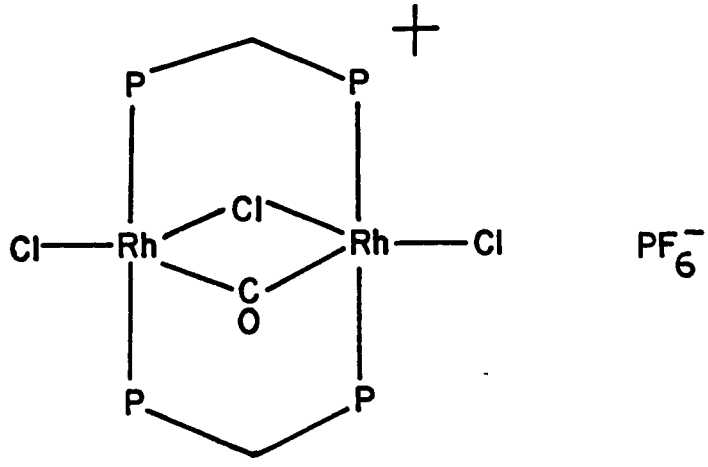
Figure 7. Cyclic voltammogram of 3 with excess TBACl.



Conditions: Conc. 5.0×10^{-4} M; 0.10 M TBAH/CH_2Cl_2; sweep rate 100 mV sec^{-1}; SCE.

Figure 8. Cyclic voltammogram of 3 with excess TBACl after oxidation at +0.70 volts.

exhibits the familiar AA'A"A'"XX' pattern indicative of a symmetrical complex ($\delta(P)$ = 9.33 ppm and $[^{1}J(RhP) + {}^{X}J(RhP)]$ = 97.7 Hz). Based on this data and a consistent elemental analysis, the green complex can be formulated as 4. This 16-electron system contains a ketonic carbonyl group having no formal metal-metal bond.



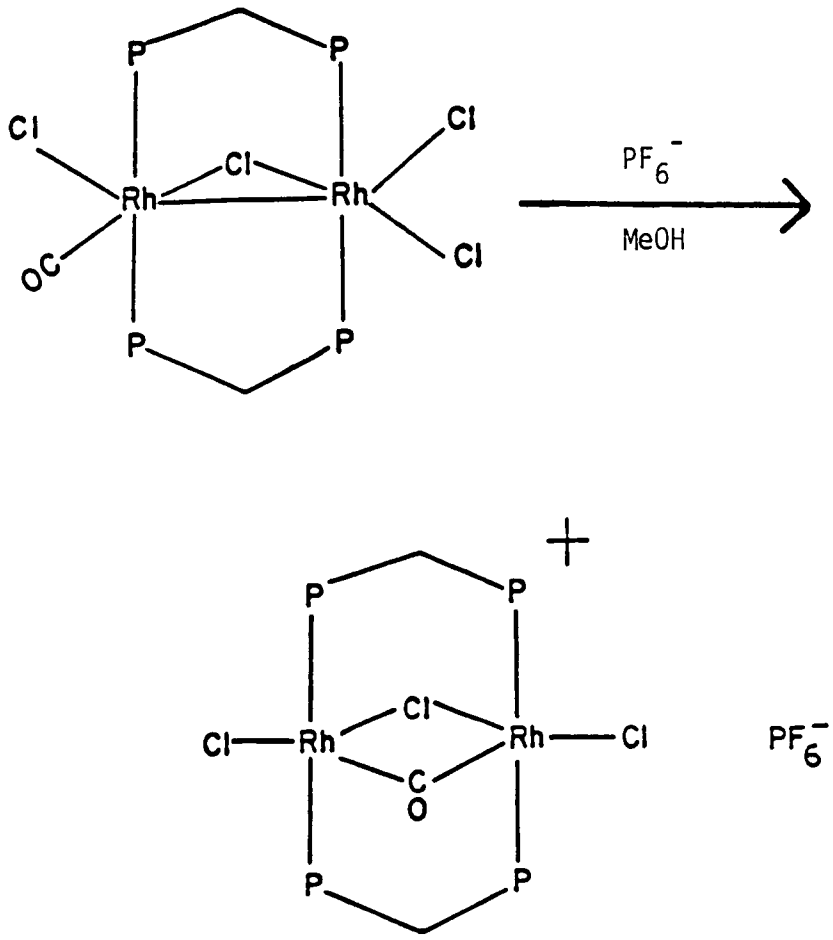
4

Performing exhaustive coulometry on the complex, trans-$Rh_2Cl_2(CO)_2(dam)_2$ in CH_2Cl_2 containing 0.1 M TBAH (or 0.1 M TBAN) and a 10-fold molar excess of TBAC, at +0.75 volts, resulted in a golden red solution. This oxidized solution was reduced in volume and acetone was added to precipitate an orange solid. Attempts to isolate an analytically pure product were futile and the product could not be characterized.

The reaction of excess TBAC with a methylene chloride solution of 4, followed by the addition of ether, produces a brown solid that features a terminal carbonyl stretching frequency at 2028 cm^{-1} (s) with no indication of the PF_6^- counter ion. The $^{31}P\{^{1}H\}$ NMR spectrum shows an NMR pattern that is not consistent with an

AA'A"A'"XX' spin system. The pattern is likely that of a AA'BB'XY system (Figure 9). The values of the coupling constants and $\delta(P)$ can only be determined by NMR computer simulation. The addition of TBAH (1:1 mol ratio) to a CH_2Cl_2 solution of the brown complex, $[Rh_2Cl_3(CO)(\mu\text{-}Cl)(dpm)_2]$, 5, followed by the addition of methanol produces the green complex, 4 (illustrated in Scheme II).

Scheme II



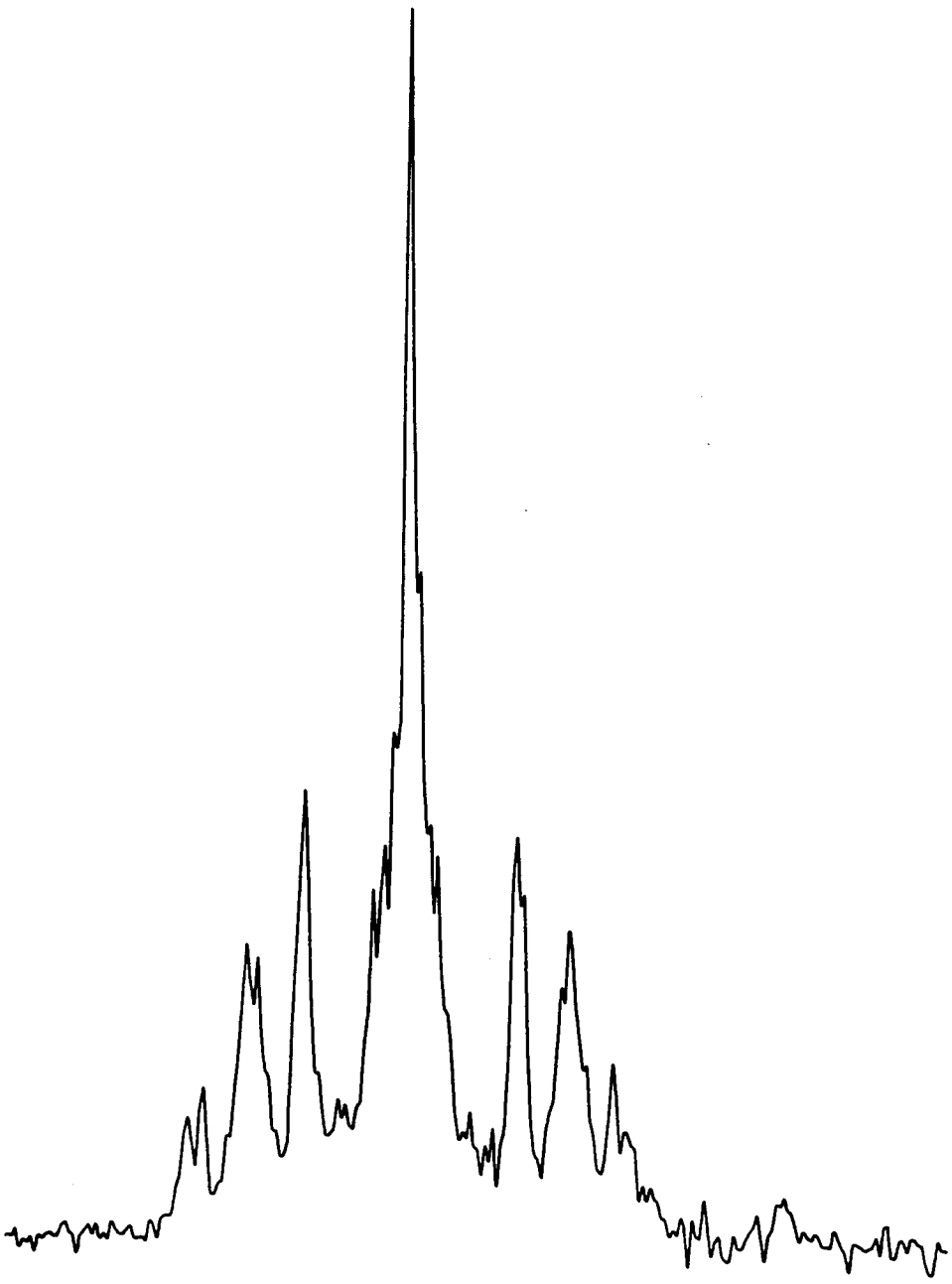


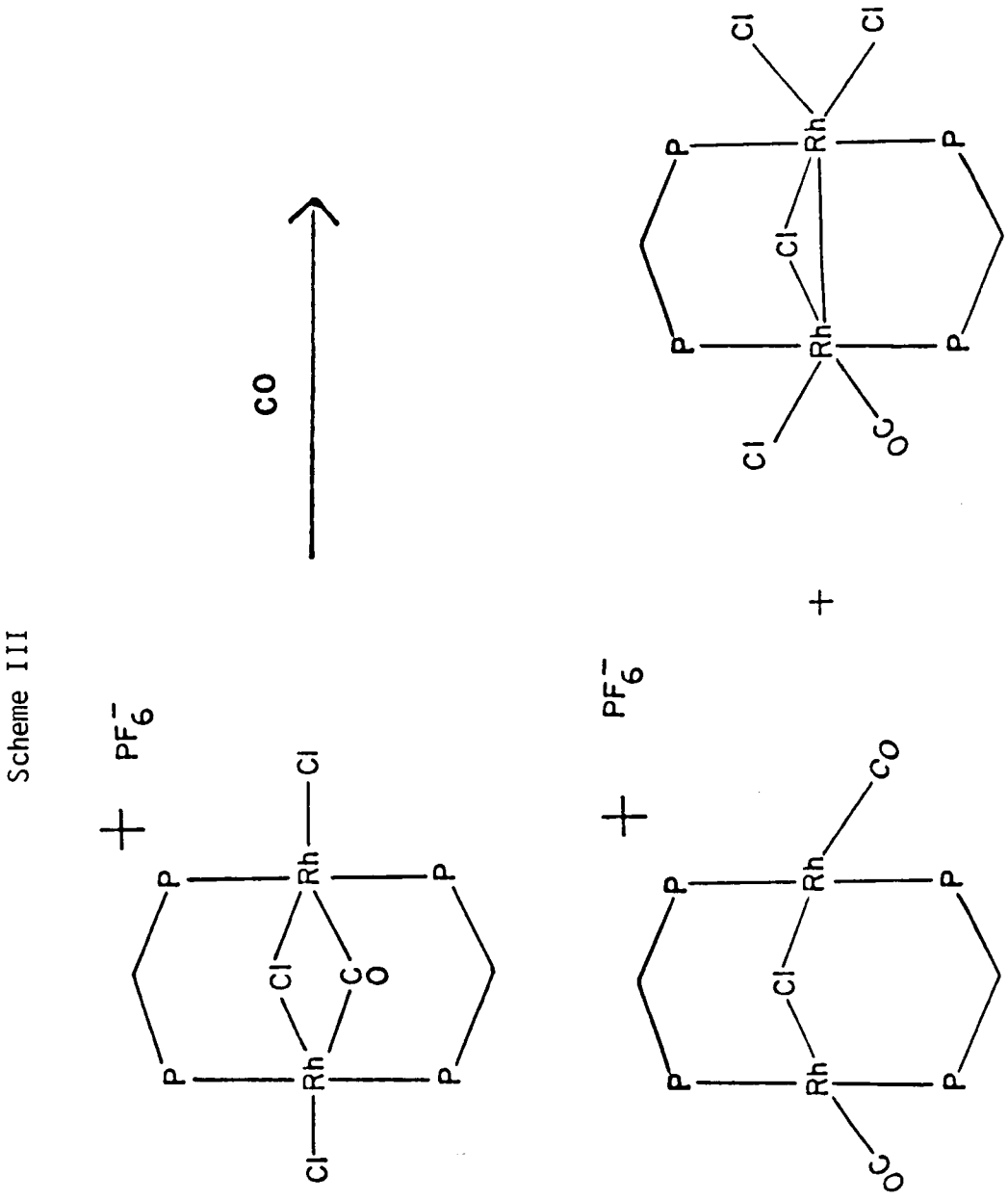
Figure 9. The $^{31}P\ \{^{1}H\}$ NMR spectrum of $Rh_2Cl_3(CO)(\mu\text{-}Cl)(dpm)_2$, 5.

Elemental analysis is consistent with the formulation of the brown complex as $Rh_2Cl_3(CO)(\mu\text{-}Cl)(dpm)_2$, 5. It is assumed to be a stable 18-electron system having a metal-metal bond with one of the Cl^- in the bridging position.

When carbon monoxide is bubbled through a CH_2Cl_2 solution of 4, the green solution turns brown to red to finally a yellow-orange color within 5 minutes. The slow diffusion of ether into the solution over a period of a few days resulted in the formation of needle-like orange crystals and octahedral black crystals which are easily separated from each other (reaction is illustrated in Scheme III). The orange crystals featured two terminal carbonyl stretching frequencies at 1994 cm^{-1} (sh) and 1978 cm^{-1} (s). The IR spectrum also shows PF_6^- peaks at 839 cm^{-1} (s) and 560 cm^{-1} (m). In addition to $^{31}P\{^1H\}$ NMR and elemental analysis, all data for the orange crystals proved to be identical to that for the A-frame complex $[Rh_2(CO)_2(\mu\text{-}Cl)(dpm)_2]PF_6$, 2.

The black crystals feature a single peak for $\nu(CO)$ at 2028 cm^{-1} (s) which is indicative of a terminal CO. The UV-Vis spectrum features two bands at 383 nm (λ_{max}) and 303 nm (λ_{max}), and the $^{31}P\{^1H\}$ NMR spectrum proved to be identical to the spectra recorded for the brown complex, 5. Elemental analysis proved to be consistent with this formulation.

Scheme III



CHAPTER V

CONCLUSIONS

This investigation has utilized various spectroscopic techniques to characterize some new dinuclear Rh(I) A-frame complexes that incorporate a triazolate anion or a pyrazolate derivative in the bridgehead position. We have shown that these complexes can easily undergo oxidative-addition and substitution reactions with various halogens. In particular, it was shown that the 3,5-DMP and pz complexes react with Br_2 and Cl_2 to yield complexes that are substituted with Br or Cl at the 4-position of the pyrazolate ring. Although this type of reaction is relatively rare with dinuclear rhodium complexes, it is not unprecedented. In 1984 Atwood synthesized and characterized a diiridium complex, $[Ir(PPh_3)(CO)(Cl)(4\text{-}Cl\text{-}pz)]_2$, that incorporates a chloride atom at the 4-position of the pyrazolate ring.[36] In contrast, the analogous reaction with Br_2 yielded the complex, $[Ir(PPh_3)(CO)(Br)(\mu\text{-}pz)]_2$, with no bromination of the ring.

The electrochemical investigations on the complexes, 6-9, suggests a quasi-reversible electron transfer process. Electrochemical studies to date do not allow one to distinguish whether the electron is being removed from the metal center or the heterocyclic ring. Further studies, including ESR and Raman experiments, are needed to resolve this issue.

Electrochemical oxidation of 3 in the presence of excess chloride led to some interesting chemistry, including the isolation of a green complex, 4, containing a ketonic carbonyl ligand and a bridging chloride ligand. One interesting and puzzling aspect associated with this green complex is the fact that it cannot be produced until methanol is added to the oxidized solution.

We have shown that the reaction of the green complex, 4, with CO followed by the slow diffusion of ether into the solution leads to the formation of black and orange crystals, 5 and 2, respectively. This mixture of Rh(I)-Rh(I) and Rh(II)-Rh(II) dimers are generated by simultaneous substitution and addition reactions.

In our studies we have shown that the electrochemical nature of A-frame complexes is dependent on the existing inner and outer sphere ligands. With the number of A-frame complexes that have been synthesized recently, this study has only scratched the surface. Further investigations are presently being conducted by other members of the research group.

LIST OF REFERENCES

LIST OF REFERENCES

1. M. Cowie, T. G. Southern, Inorg. Chem., 21, 246 (1982).
2. C. P. Kubiak, R. Eisenberg, J. Am. Chem. Soc., 99, 6129 (1977).
3. C. P. Kubiak, R. Eisenberg, Inorg. Chem., 19, 2726 (1980).
4. M. M. Olmstead, H. Hope, L. S. Benner, A. L. Balch, J. Am. Chem. Soc., 99, 6129 (1977).
5. M. Cowie, J. T. Mague, A. R. Sanger, J. Am. Chem. Soc., 100, 3628 (1978).
6. M. Cowie, Inorg. Chem., 18, 286 (1979).
7. J. T. Mague, A. R. Sanger, Inorg. Chem., 18, 2060 (1979).
8. M. Cowie, S. K. Dwight, A. R. Sanger, Inorg. Chem. Acta, 31, L407 (1978).
9. A. R. Sanger, J. Chem. Soc., Dalton Trans., 228 (1981).
10. M. Cowie, S. K. Dwight, Inorg. Chem., 18, 2700 (1979).
11. A. L. Balch, B. Tulyathan, Inorg. Chem., 16, 2840 (1977).
12. J. T. Mague, S. H. DeVries, Inorg. Chem., 19, 3743 (1980).
13. W. A. Fordyce, G. A. Crosby, J. Am. Chem. Soc., 104, 985 (1982).
14. J. T. Mague, S. H. DeVries, Inorg. Chem., 21, 1632 (1982).
15. M. Cowie, S. K. Dwight, Inorg. Chem., 19, 209 (1980).
16. C. P. Kubiak, R. Eisenberg, J. Am. Chem. Soc., 102, 3637 (1980).
17. C. Woodcock, R. Eisenberg, Inorg. Chem., 24, 1285 (1985).
18. C. P. Kubiak, C. Woodcock, R. Eisenberg, Inorg. Chem., 21, 2119 (1982).
19. M. Cowie, S. K. Dwight, Inorg. Chem., 19, 2500 (1980).
20. S. P. Deranizagala, K. R. Grundy, Inorg. Chem., 24, 50 (1985).
21. M. Cowie, T. G. Southern, J. Organometal. Chem., 193, C46 (1980).

22. M. Cowie, R. S. Dickson, Inorg. Chem., 20, 2682 (1981).

23. D. Womack, M. S. Thesis, The University of Tennessee, Knoxville, 1981.

24. A. L. Balch, J. Am. Chem. Soc., 98, 8049 (1976).

25. A. L. Balch, J. W. Labadie, G. Delber, Inorg. Chem., 18, 1224 (1979).

26. L. A. Bottomley, T. A. Hallberg, Inorg. Chem., 23, 1584 (1984).

27. F. A. Cotton, T. R. Felthouse, Inorg. Chem., 19, 323 (1980).

28. F. A. Cotton, T. R. Felthouse, Inorg. Chem., 19, 2347 (1980).

29. P. D. Enlow, C. Woods, Inorg. Chem., 24, 1273 (1985).

30. D. R. Womack, P. D. Enlow, C. Woods, Inorg. Chem., 22, 2653 (1983).

31. J. T. Mague, J. P. Mitchner, Inorg. Chem., 8, 119 (1969).

32. P. W. Tinsley, M. S. Thesis, The University of Tennessee, Knoxville, 1981.

33. L. A. Oro, D. Carmona, P. L. Perez, M. Esteban, A. Tiripicchio, M. T. Camelline, J. Chem. Soc., Dalton Trans., 973 (1985).

34. R. W. Murray, C. N. Reilley, "Electroanalytical Principles." New York: Interscience, 1963.

35. R. S. Nicholson, Anal. Chem., 37, 1351 (1965).

36. J. L. Atwood, K. A. Beveridge, G. W. Bushell, K. R. Dixon, D. T. Eadie, S. R. Stobart, M. J. Zaworotko, Inorg. Chem., 23, 4050 (1984).

VITA

Christopher James Janke, the third of five children, was born in King of Prussia, Pennsylvania, on April 6, 1960. In Greensboro, North Carolina he attended Saint Pius X and Kiser Junior High School, and subsequently graduated from Grimsley Senior High School in June 1978. After five years at Appalachian State University, he received a B. S. in Chemistry in May 1983. He then accepted a Graduate Research-Teaching Assistantship from The University of Tennessee, Knoxville. He was awarded the M. S. in Chemistry from The University of Tennessee, Knoxville in March 1986.

In June 1986 he was married to his lovely fiancée, Pamela Gail Burgess, in Oak Ridge, Tennessee.